GA-C16190

STRUCTURAL SAFETY EVALUATION OF A CRACKED FORT ST. VRAIN CORE SUPPORT BLOCK DURING LOFC WITH FIREWATER COOLDOWN

by

JOE KIM and RUSSELL E. VOLLMAN

Prepared under
Purchase Order N-2938
For Public Service Company of Colorado

POOR ORIGINAL

GENERAL ATOMIC PROJECT 2970
DECEMBER 1980

GENERAL ATOMIC COMPANY

8102100 350

GA-C16190

STRUCTURAL SAFETY EVALUATION OF A CRACKED FORT ST. VRAIN CORE SUPPORT BLOCK DURING LOFC WITH FIREWATER COOLDOWN

AUTHORS

Joe Kim and
Russell E. Vollman   Joe K. Kim
Russell E. Vollman

REVIEWER

Fu H. Ho   Fu Hua Ho 12/23/80

APPROVALS

H. Jones
Manager, Core Design   H. Jones 12.23.80

W. Simon
Manager, Core Engineering   H. Jones 12.23.80 for W.S.

G. Bramblett/J. Lopez
Project Manager, FSV Project   12/23/80 / G. Bramblett 12/30/80

DECEMBER 1980

POOR ORIGINAL

SUMMARY

The purpose of this study is to determine the safety consequences of a cracked core support block on the subsequent cooldown of the FSV-HTGR during a hypothetical LOFC with firewater cooldown after a 90 minute delay. A very conservative cracking pattern is derived from thermal stress fields predicted by LASL personnel (Ref. 1) from ORNL ORECA calculations of core thermal performance during the hypothetical event.

The results show that the cracked core support block remains in place with minimal disarray of the fuel columns.

It is concluded that the cracked core support block does not interfere with safe cooldown of the reactor core.

CONTENTS

FIGURES

TABLES

1. INTRODUCTION

During operation of the Fort St. Vrain High Temperature Gas-Cooled Reactor (HTGR) a Loss of Forced Circulation (LOFC) event could hypothetically occur. The purpose of this study is to determine the safety consequence of an LOFC with subsequent cooldown on one Pelten wheel driven circulator powered by the firewater system aided by booster pumps on a PGX graphite core support (CS) block found to experience rather high thermal stresses during the cooldown transient.

The overall graphite and coolant temperature history was predicted by Dr. Syd Ball using the ORECA code at ORNL.

The results of the above thermal analysis were used as thermal boundary conditions for a thermal stress analysis of the affected CS block by Dr. Tom Butler of Los Alamos Scientific Laboratory (LASL). The results of this analysis indicated high thermal stresses in the keyways of the CS blocks. In discussions of the results it could not be conclusively proven whether or not the possible cracks that could form would propagate leading to collapse of the CS block. Thus, it was decided to perform an analysis of the CS block to determine the consequences to the CS function of thermal stress cracking. Furthermore, as a basis for conservatism, the cracks would be assumed to propagate to a very conservative pattern that could be inferred from the stress field predicted by Dr. T. Butler.

2. GEOMETRIC CONFIGURATION

2.1. CORE SUPPORT STRUCTURE

The CS consists of the concrete CS floor, the graphite CS floor assembly, and the lateral restraint assembly. The graphite CS floor is assembled from graphite blocks and posts to provide a stable horizontal surface upon which the core and reflector rest, as shown in Fig. 1. The modular design allows for independent thermal movements between the refueling regions and the permanent side reflectors (PSR). Three core support posts support each CS block in a stool fashion. The post ends are spherical and roll on spherical cups to accommodate relative movement between the core and concrete CS floor. In this way stresses due to differential movements are eliminated.

The core and CS are restrained laterally by a steel core barrel which is keyed radially to the PCRV. The CS floor and the top of the PSR are keyed to the core barrel. In this way radial and vertical movements are permitted but not rotation about a vertical axis.

The CS posts and CS blocks will be described in more detail in the following paragraphs.

2.1.1. <u>Core Support Posts</u>

Primary functions of support posts are as follows:

1. To support the CS blocks, reactor-core, top and bottom reflectors, PSR's, and top plenum orifice elements.

2. To provide a core outlet coolant mixing plenum before distributing the gas to the heat exchangers.

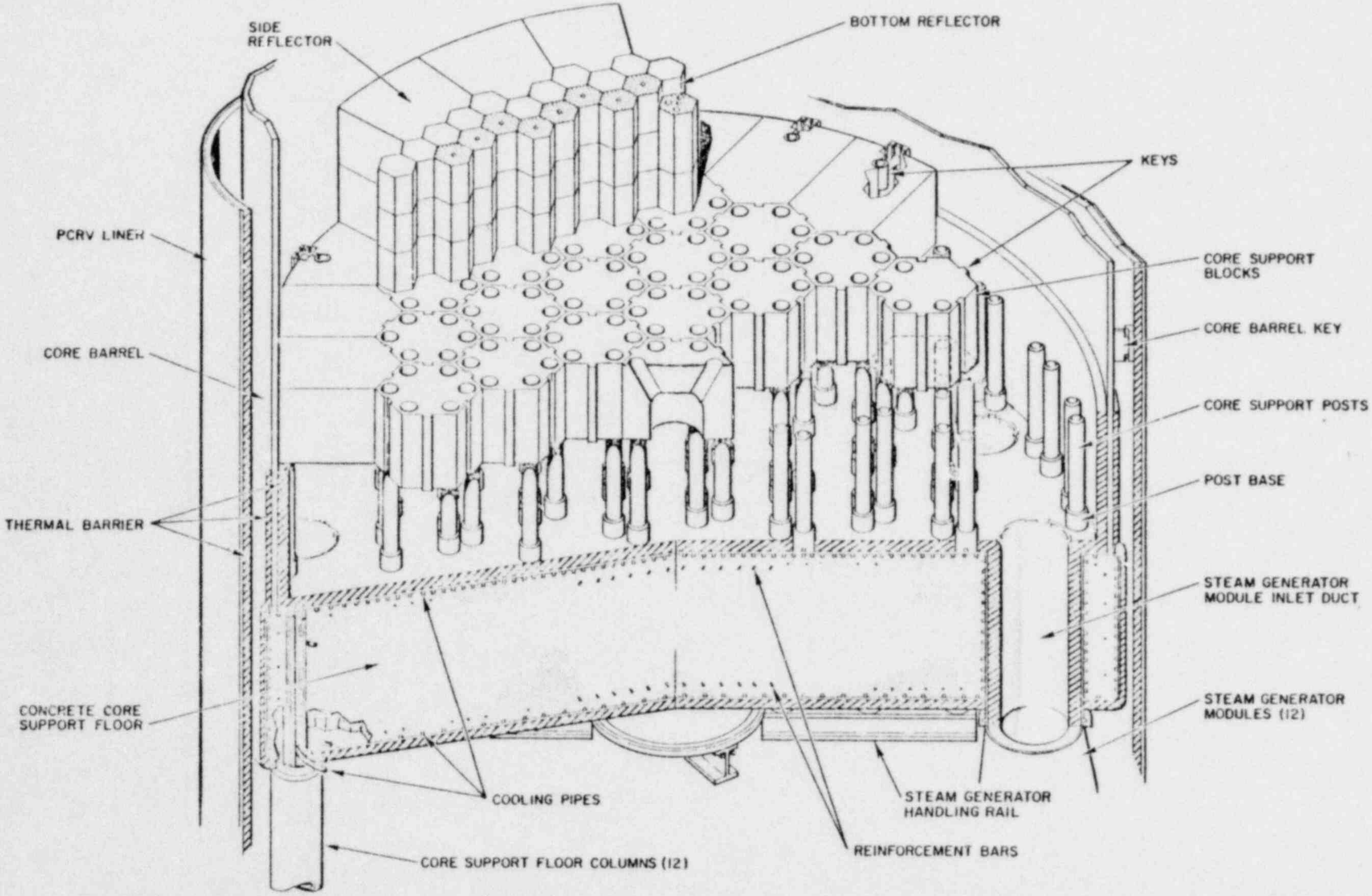

Fig. 1. Core support arrangement

The posts have hemispherical ends. This hemispherical shape allows the posts to rock in the CS blocks and lower bearing seats without bending and sliding. In this way, differential movements between the blocks and floor (Ref. 1) can be accommodated without interference.

2.1.2. Core Support Block

The primary function of the core support block is to support top and bottom reflectors, reactor-core, and top-plenum-orifice-elements. In addition, its function is to mix the core-outlet-coolant gasses exiting from a refueling region in the core-support-block and measure the refueling region coolant mixed mean outlet temperature.

Each CS block is radially keyed to the surrounding six adjacent blocks. The peripheral CS blocks are keyed to permanent-side reflector support blocks which are in turn keyed to the steel core barrel. As the core barrel radially expands due to thermal expansion, the permanent side reflector support blocks are pulled out with the core barrel. The CS blocks keyed to the PSR support blocks are also pulled out in the radial direction to take up the core barrel radial displacement. These movements result in an increase in the nominal gaps between CS blocks during 100% power normal operation. This subject will be discussed more in Section 3 on gap analysis.

3. CORE BARREL AND GAP ANALYSIS

The total gap between adjacent CS blocks is the sum of the normal-operation-gap and an additional gap due to thermal expansion of the core barrel during the LOFC.

The parameters used for gap analysis and results are summarized in Table 1.

3.1. NORMAL OPERATION GAP

The CS blocks are installed with nominal gaps between them of 0.25 in. As the core and core barrel heat up to 100% power steady state operation these gaps are estimated to grow to 0.399 in. (Refs. 2 and 3).

3.2. CORE BARREL TEMPERATURE DURING LOSS OF FORCED CIRCULATION EVENT

Figure 2, taken from the FSV FSAR (Ref. 4), illustrates the core barrel temperature near core support keys and core midplane. It also shows that the core barrel temperature near the support keys reaches 1150°F (621°C) 10 hours after LOFC occurred. The core-barrel-temperature reaches a maximum (≈2300°F or 1260°C) near core midplane about 150 hours after the start of the LOFC accident.

To be conservative in the gap prediction, the core barrel thermal expansion is calculated using the maximum temperature during LOFC event. This surely yields an upper bound value for the gap estimate.

3.3. GAP DUE TO CORE BARREL THERMAL EXPANSION

The radial core barrel thermal expansion is 2.09 in. based on the 2300°F core barrel temperature. This expansion is divided into four gaps

TABLE 1
SUMMARY OF CORE BARREL AND GAP ANALYSIS

Thermal expansion coefficient at 2500°F (ASTM 387 Grade B 1.0 Cr-0.5 Mo alloy and carbon steel)	$\approx 8 \times 10^{-6}$/°F
Temperature of core barrel at normal operation	750°F
Maximum temperature of core barrel at LOFC/FWCD	2300°F
Diameter of core barrel (Ref. 3)	28.4 ft
Radial thermal expansion of core barrel	$\approx$ 2.1 in.
Maximum gap between CS blocks at normal operation	$\approx$ 0.40 in.
Maximum gap between CS blocks used for this analysis	$\approx$ 1.0 in.

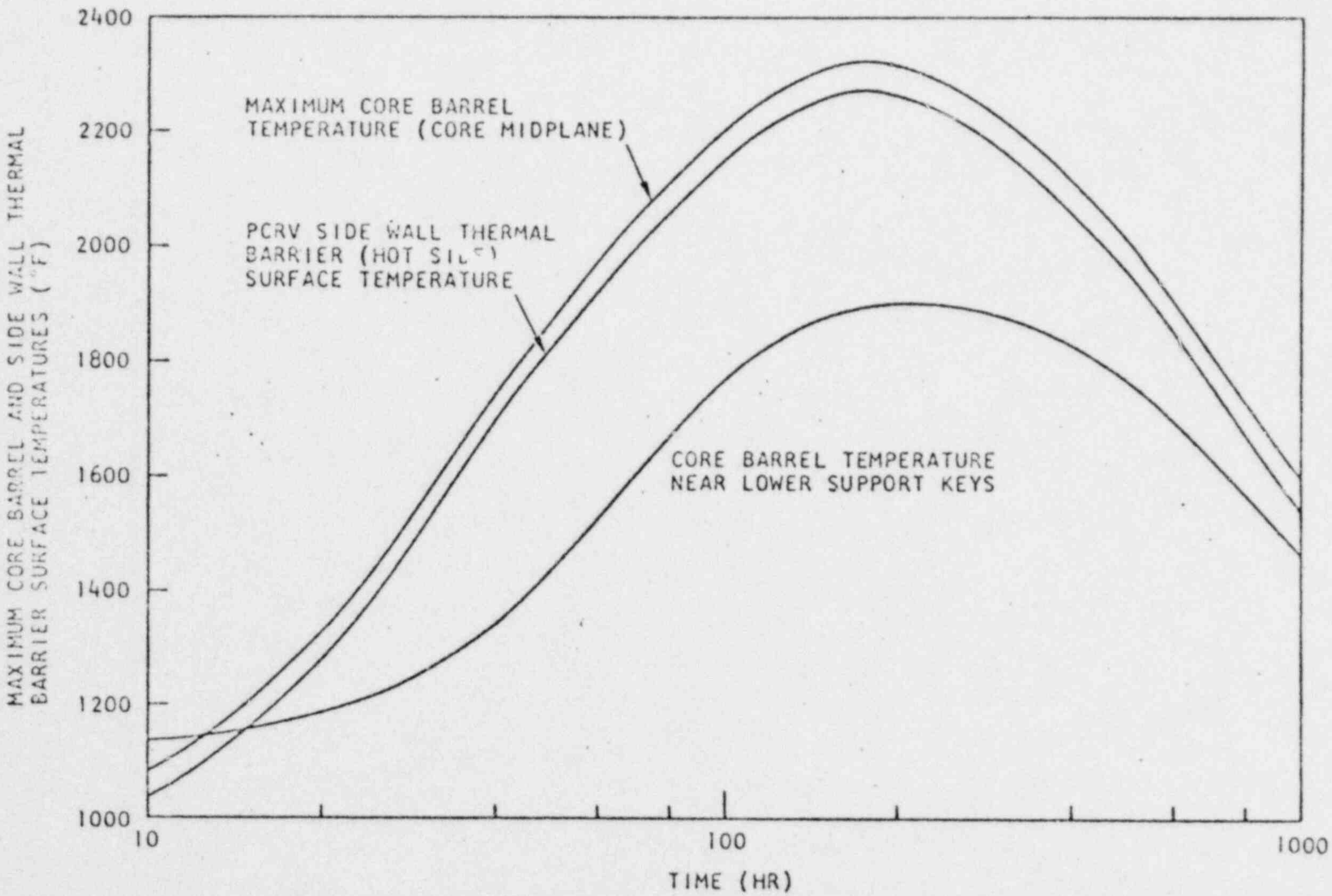

Fig. 2. Core barrel temperatures and maximum PCRV side wall thermal barrier surface temperatures during accident (Ref. 5)

from the center of core to the PSR (see Fig. 3) resulting in a 1.0 in. gap between blocks. Figure 4 shows the result of gap analysis for the normal operation and LOFC.

Further detailed calculation is presented in Appendix G.

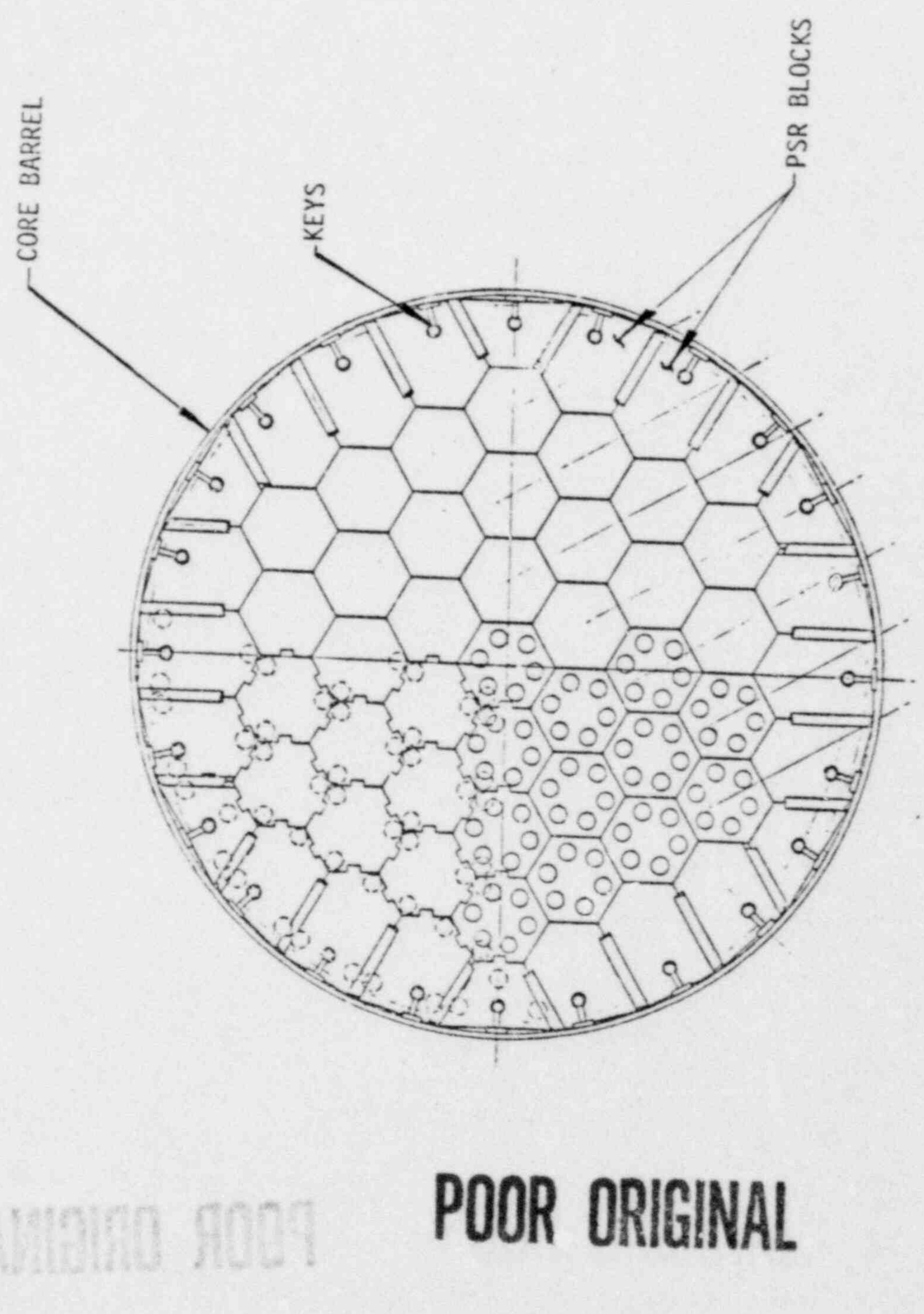

Fig. 3. Core support floor configuration

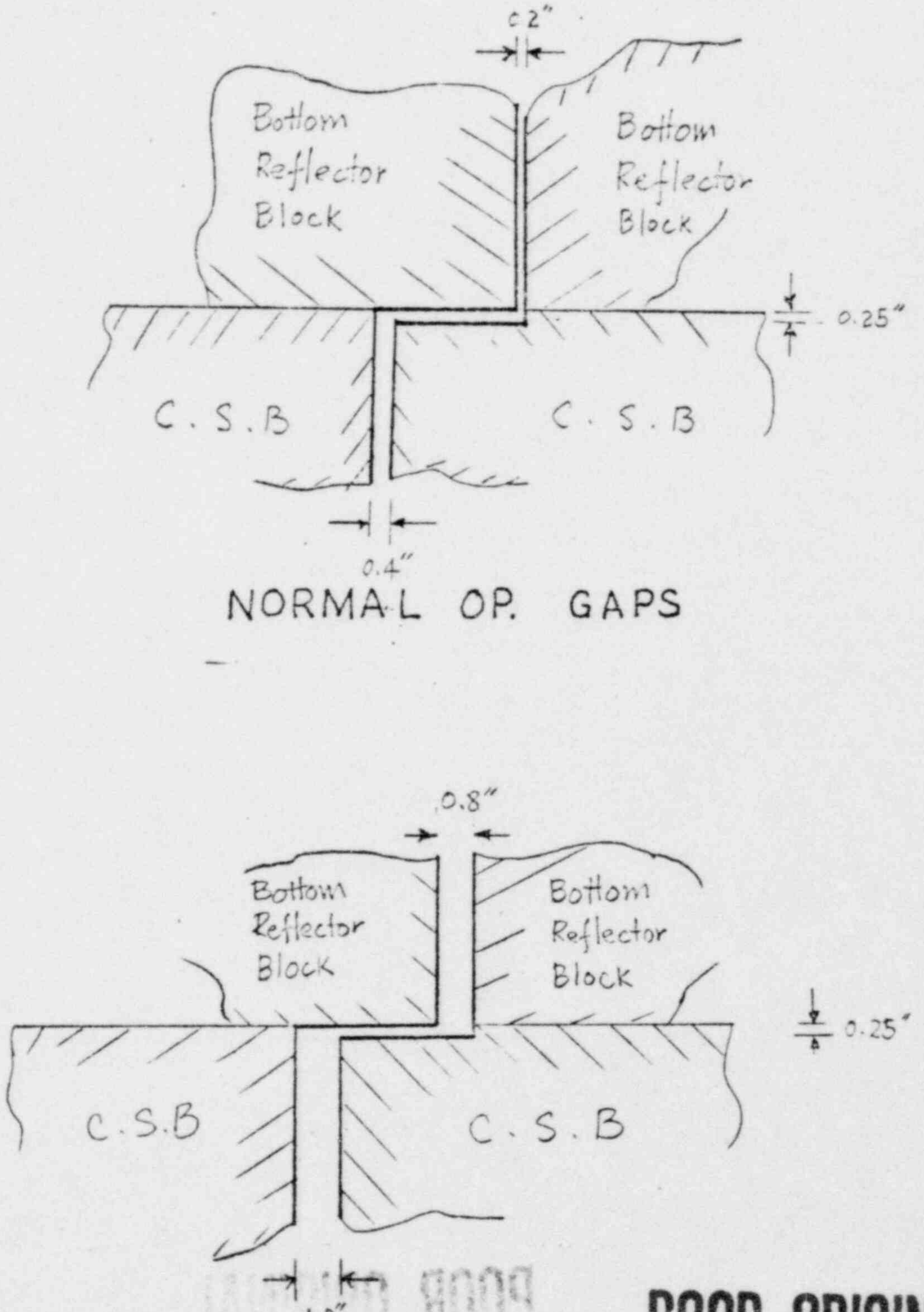

Fig. 4. LOFC gaps before cracking

4. CORE SUPPORT BLOCK CRACKING ANALYSIS

4.1. ASSUMPTIONS OF ANALYSIS

The following assumptions were made in this analysis:

1. Cracks start at the corners of the keyways and propagate to coolant channels. This assumption is based on the results of the thermal stress analysis performed by LASL personnel which predicted maximum tensile stresses of 1600 psi in the corner of the top of the keyway. The maximum principal stress drops rapidly away from the corner to about 300 psi then rises again towards the edge of the coolant hole to about 600 psi.

2. The web between coolant holes cracks along the minimum ligament thickness. In order for the block to break into more than one piece the webs between coolant holes must crack. It is reasonable to assume that cracking will occur at a location along the plane of minimum web thickness.

3. Both frictionless and frictional contact surfaces are analyzed separately. Contact surfaces without friction allow surfaces to slide relative to one another so that pieces of the CS block will achieve their maximum movements before they jam between adjacent CS blocks. Contact surfaces with friction forces will yield the proper equilibrium position. The problem is then bounded by these analyses.

4. Gaps between blocks are based on 2300°F core barrel temperature. This allows maximum size gaps to form between blocks so that the CS block disarray is a maximum resulting in greatest fuel column

movements. The assumption is that if the region support holds together for this upper bound gap size then it will also hold together for lower core barrel temperatures.

5. Gaps between core support blocks are uniformly distributed. This is a reasonable assumption since the blocks are designed to move along the key-keyway constraints between blocks. The core barrel pulls radially outward uniformly. There are gaps between keys and keyway of about 0.060 in. which will result in some non-uniformity of the gaps in question. However, the very large gaps resulting from the 2300°F core barrel should overshadow any tolerance buildup.

4.2. CRACKING PATTERN

The fracture pattern scenario is divided into four steps. The four steps are as follows:

1. The crack initiates at one corner of the keyway due to the presence of thermal stress exceeding the ultimate tensile strength of PGX graphite as shown in Fig. 5. The crack initiates here (points A in Fig. 5) because this is where the coldest adjacent block is located creating the highest thermal stress.

2. The initiated crack is assumed to propagate to the coolant channel and vertically downward to the bottom of the core support block. This process is shown in Fig. 6. Actually it is not clear that the crack will propagate since it is initiated in a rapidly decaying tensile stress field.

3. Carrying the scenario farther it is assumed that the other keyways in the same block also crack, even though they are at a lower stress value. At this stage, all cracks have initiated from the key-way-corners and propagated to the coolant channels and to

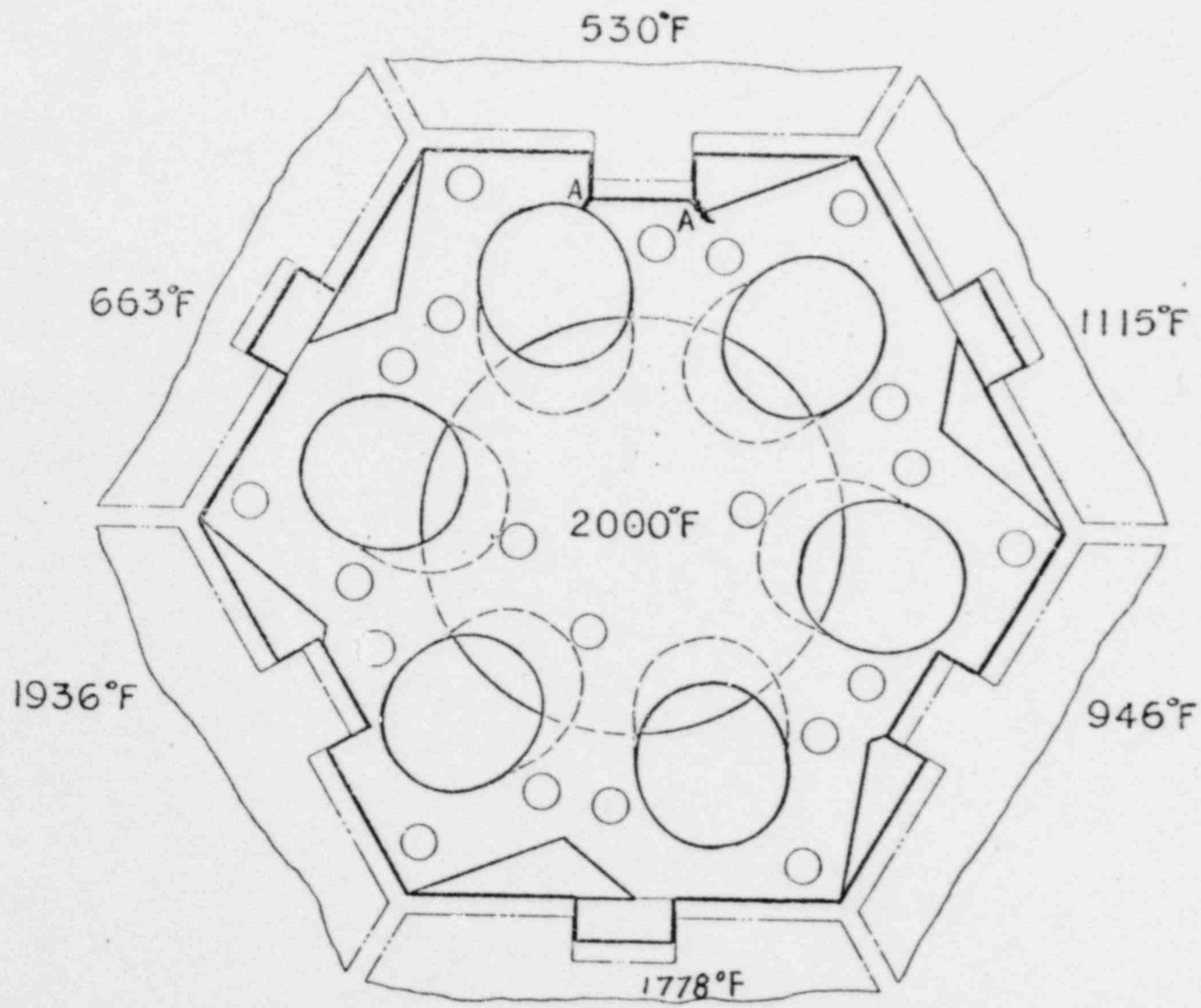

Fig. 5. Cracking pattern of core support block

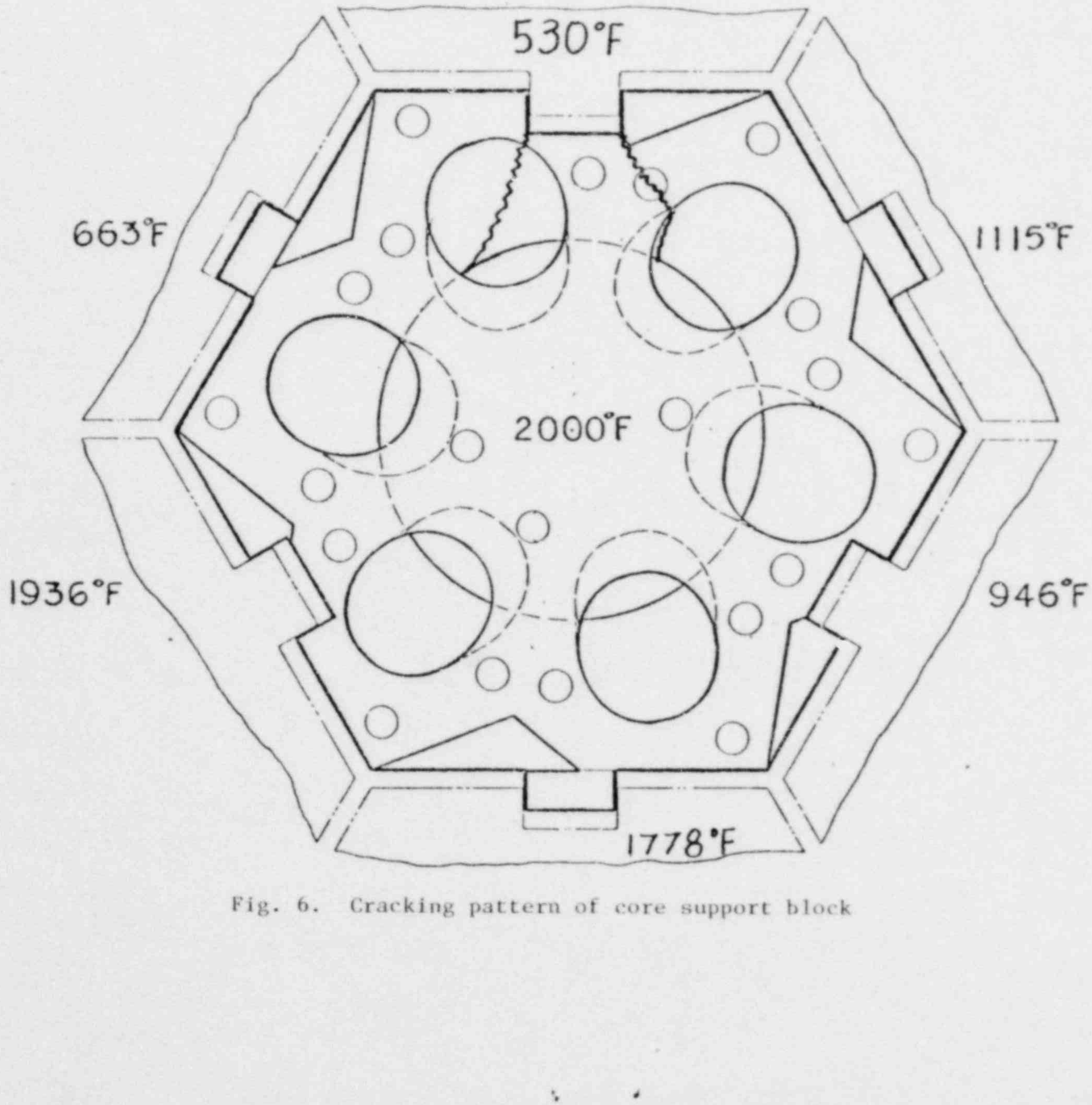

Fig. 6. Cracking pattern of core support block

POOR ORIGINAL

the bottom of the block (Fig. 7). Thus, the center control-rod-column is supported solely by webs between coolant channels of the support block.

4. The center control rod column and other surrounding standard fuel columns impose bending and shear on the webs. That resulting stress state is assumed to induce tensile stresses large enough to exceed the ultimate strength of PGX graphite. The webs crack, as shown in Fig. 8, resulting in the block breaking into four pieces. The completed cracking pattern is shown in Fig. 9. Figure 10 shows the block before cracking for comparison with the cracked block.

It is to be noted that the core outlet thermocouple assemblies are assumed structually non-significant duing this hypothetical accident. In addition, the thermocouple graphite sleeve breaks in two as the center of the block drops.

Upon completion of step 4, the control rod column and the center piece of CS block move downward 2.63 in. pushing the post pieces 1 in. in the radially outward direction until flat face to face contact occurs with the adjacent blocks. Slight rotation of the block pieces occur within the limits of the key-keyway dimensions ultimately resulting in static equilibrium of the assembly. The dislocation of the center piece is illustrated in Fig. 9. Kinematics of the cracked CS block is shown in detail in Appendix B.

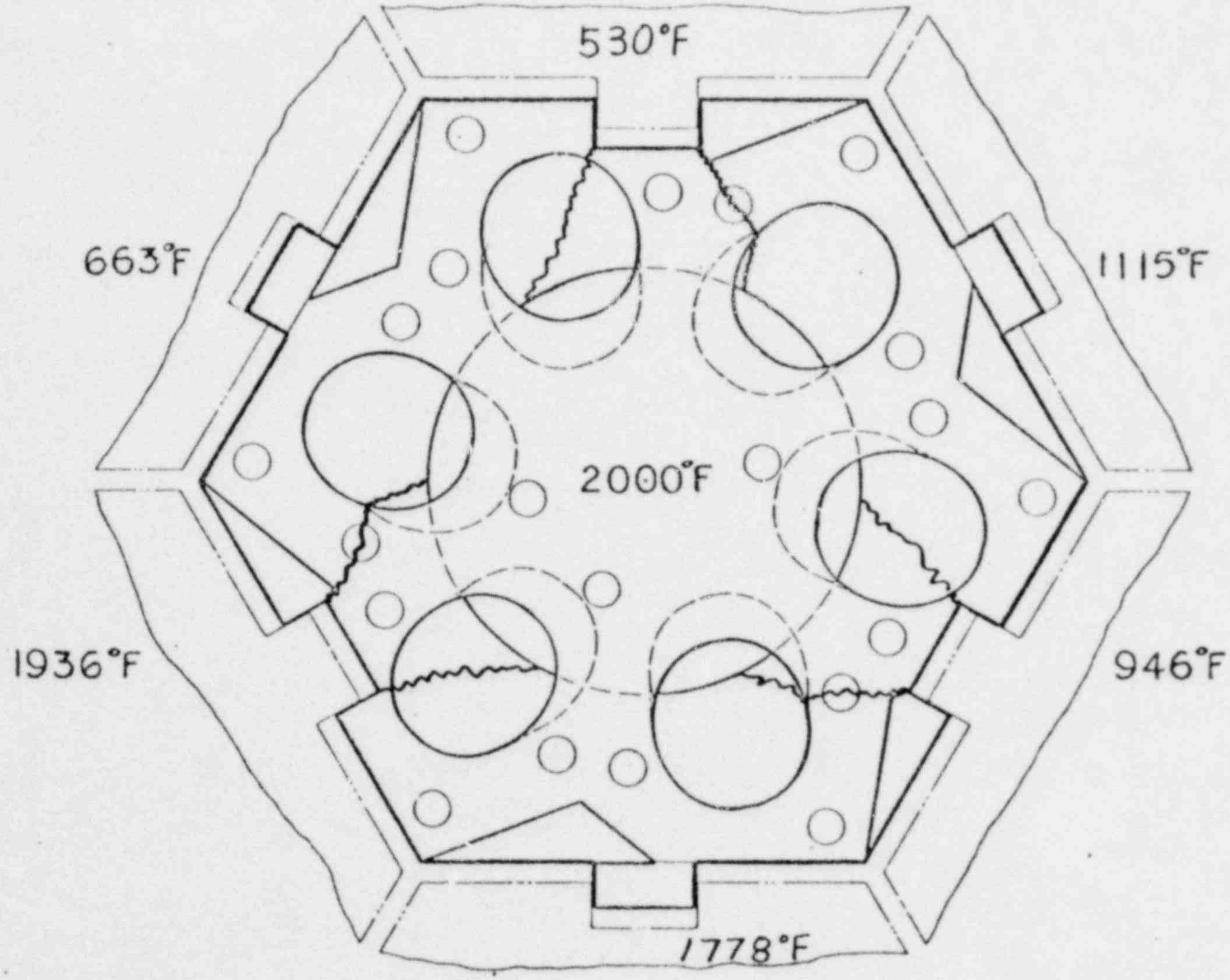

Fig. 7. Cracking pattern of core support block

POOR ORIGINAL

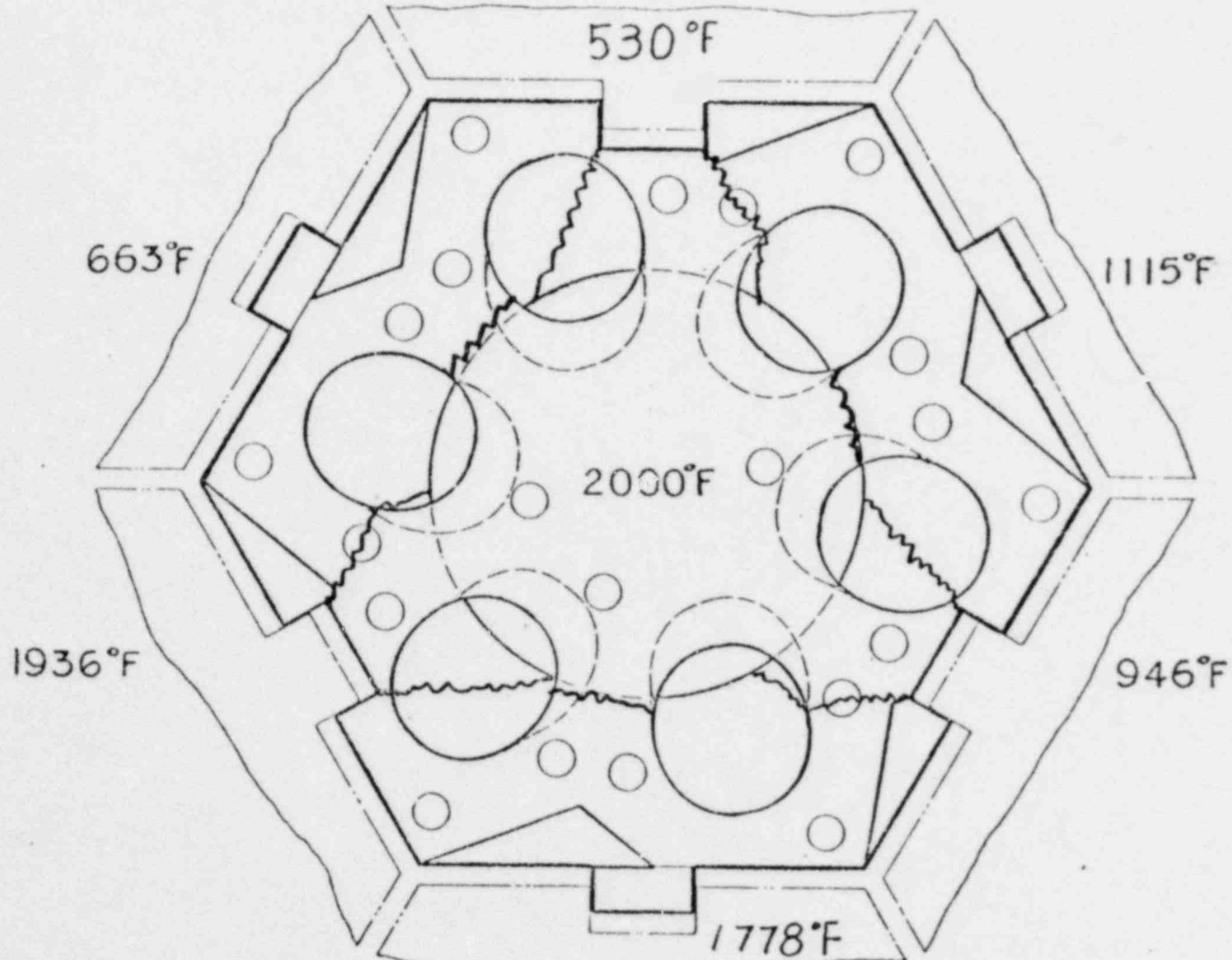

Fig. 8. Cracking pattern of core support block

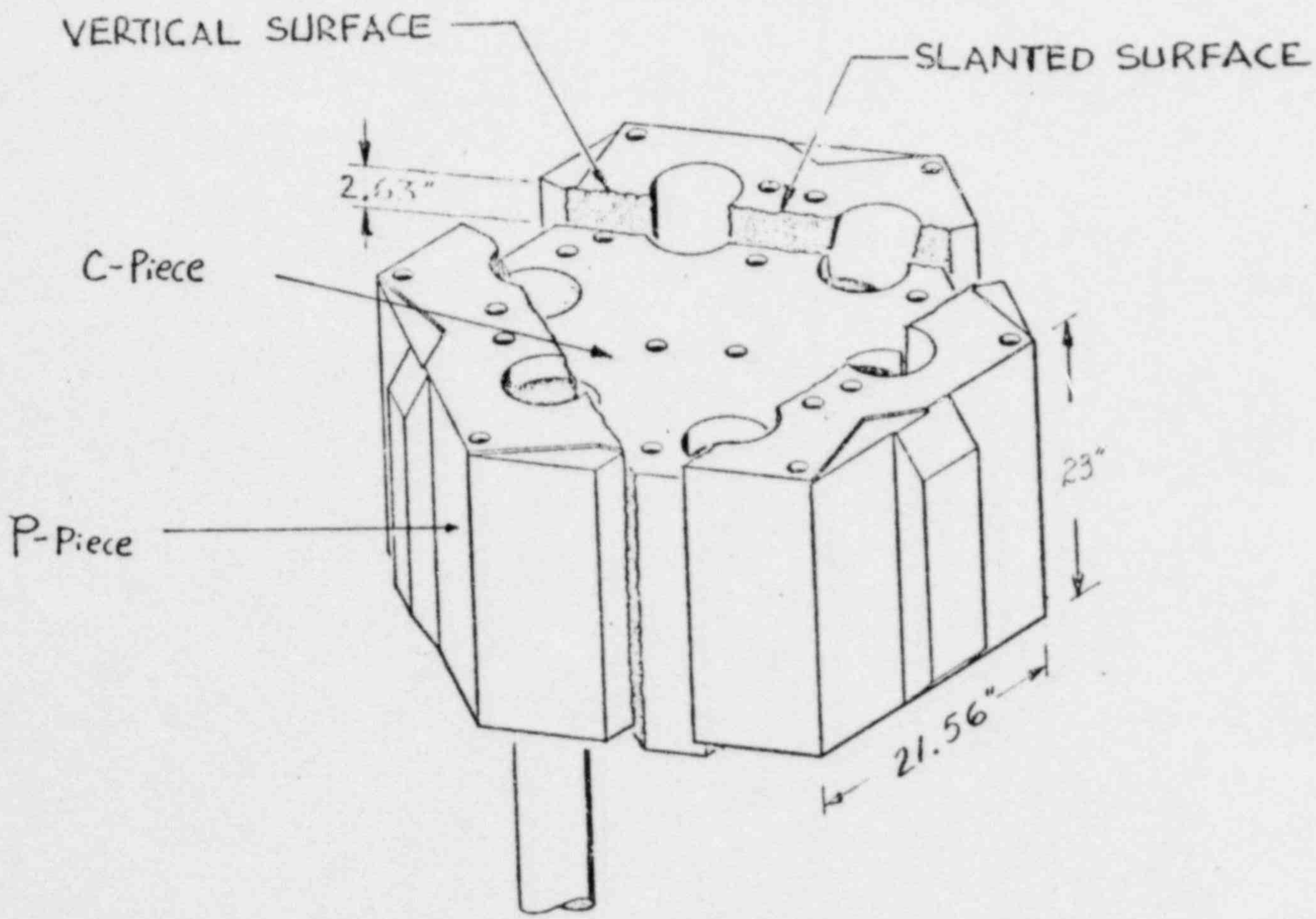

Fig. 9. Cracked core support block

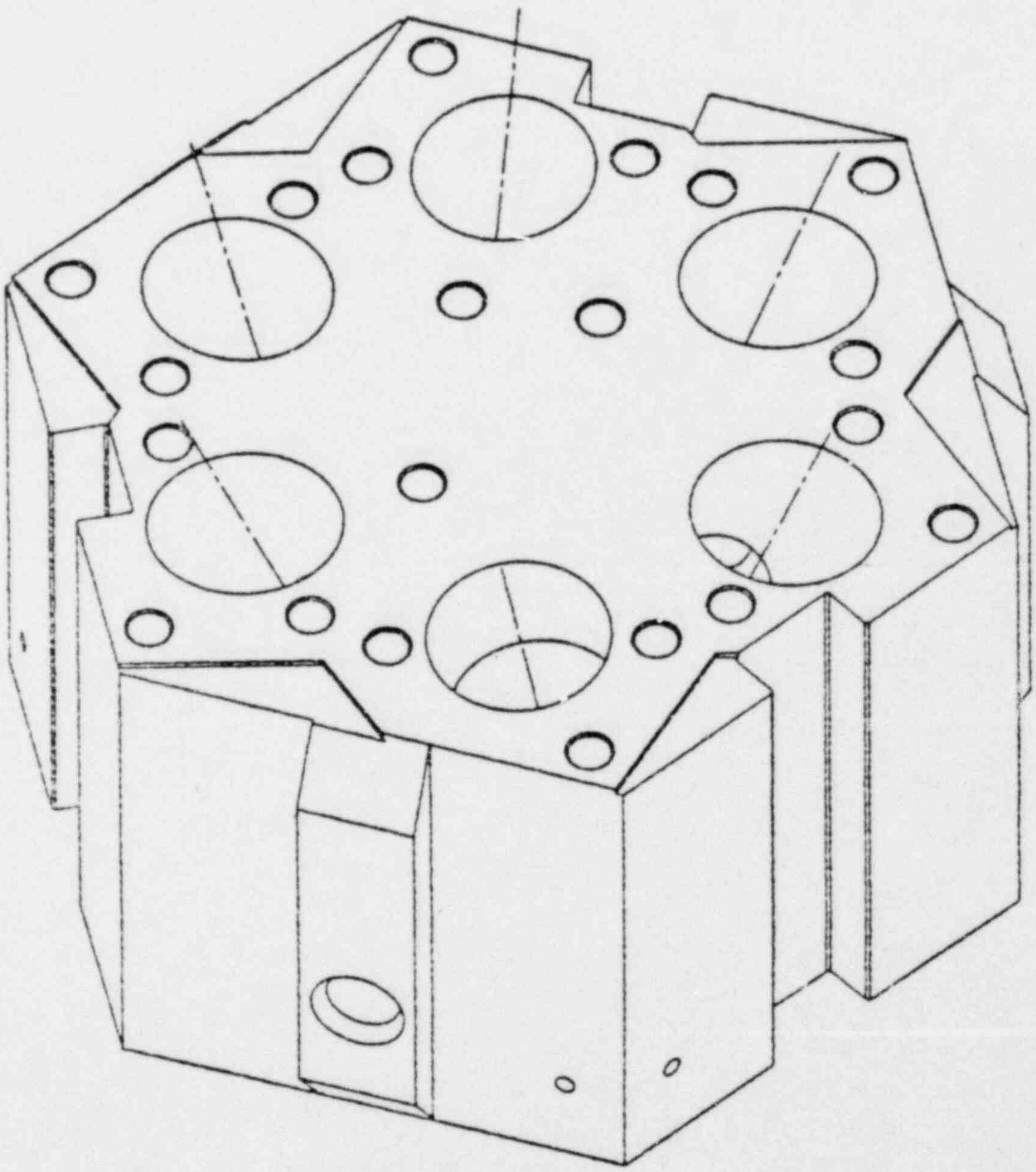

Fig. 10. Core support block before crack

POOR ORIGINAL

5. ANALYSIS OF CRACKED BLOCK - WITH KEYS

At the end of the cracking scenario outlined in the previous section the core support block is left in four pieces as shown in Fig. 9. As the pieces rotate within the confine of the key-keyway system the keys are loaded by a force couple at the top and bottom of the key. Once the key jams in the keyway no further relative rotation can occur. The static analysis that follows presents calculated forces on the block and resultant stresses.

5.1. FORCE EQUILIBRIUM

The loads on the CS block pieces come from the weight of the fuel element, flow control valve, and the weight of the block pieces themselves. Each outer fuel column weighs 2550 lb which the center control rod column weighs 2215 lb.

Figure 11 shows all static equilibrium forces without friction forces acting on the cracked core support block. The detailed steps to obtain this result are given in Appendix E. In addition friction forces are considered for two special cases in order to compare the results with friction and those without friction. The cases are as follows.

1. Complete flat face-to-face contact between cracked and adjacent CS blocks. Figure 12 shows the results of case 1.

2. Contact between the cracked CS block and an adjacent CS block occurs at the top of the blocks. The results of this case are shown in Fig. 13.

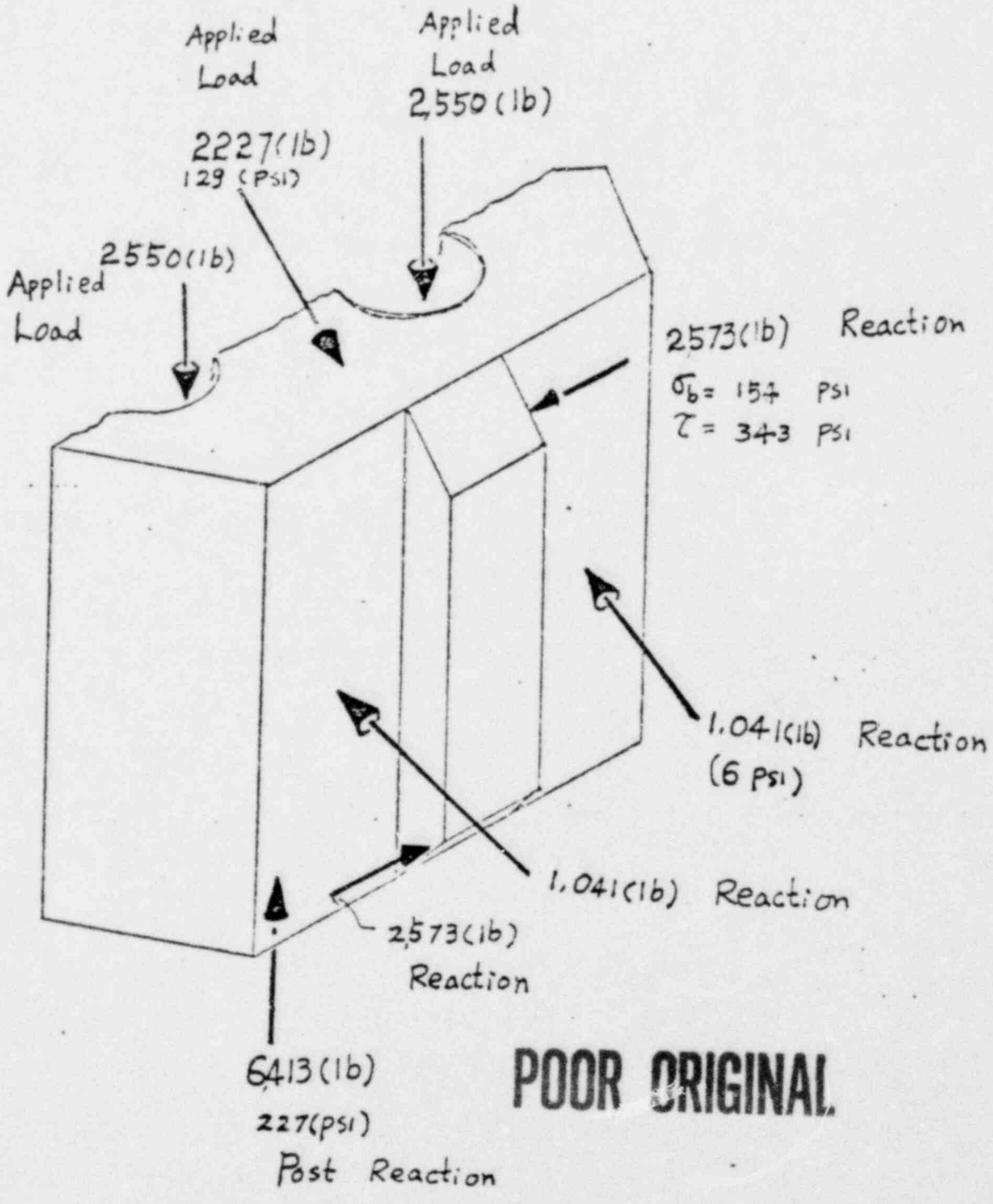

POOR ORIGINAL

Fig 11. Loads on cracked block before key sheared off-friction forces are neglected

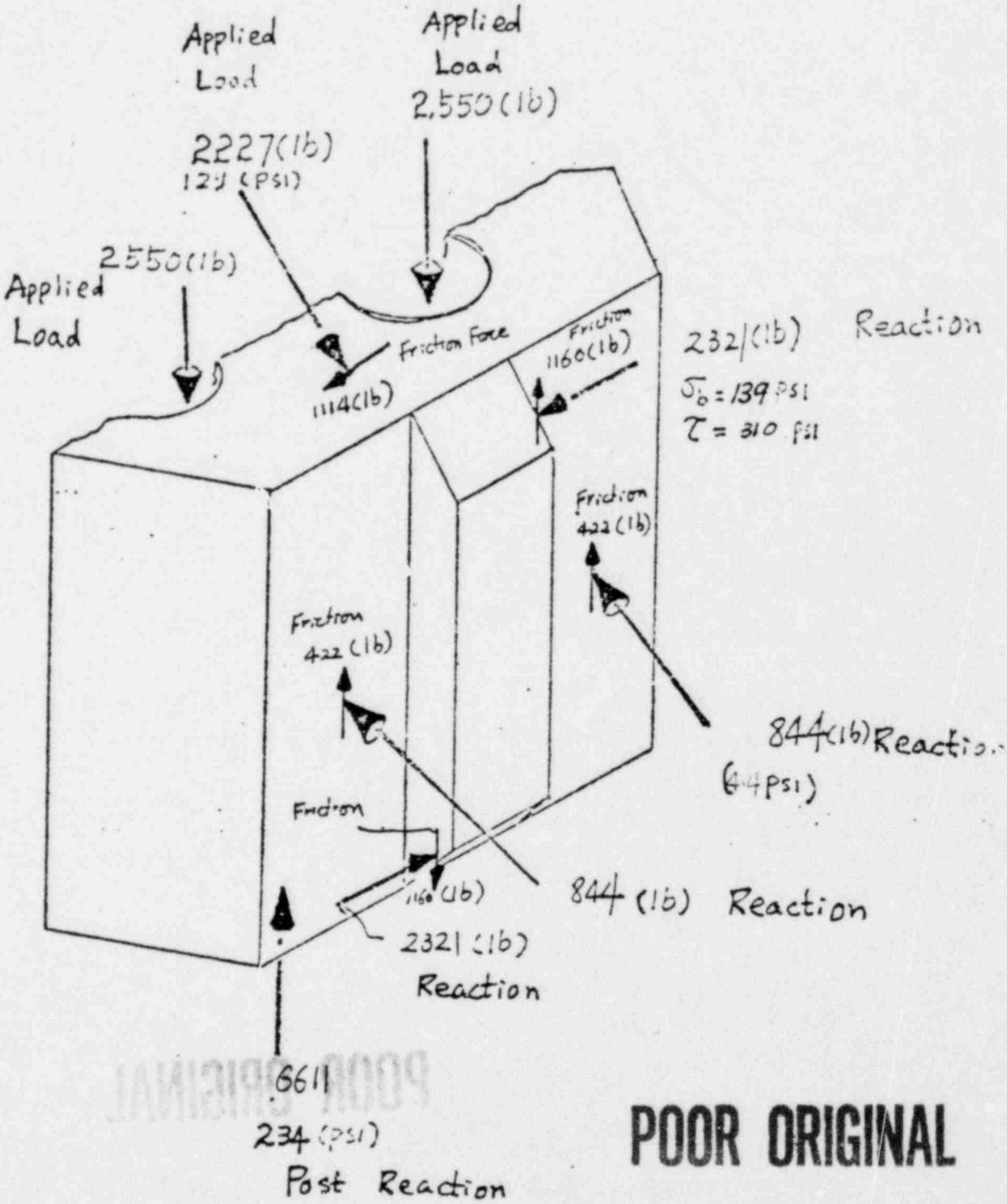

POOR ORIGINAL

Fig. 12. Loads on cracked block with friction forces before key sheared off - case 1

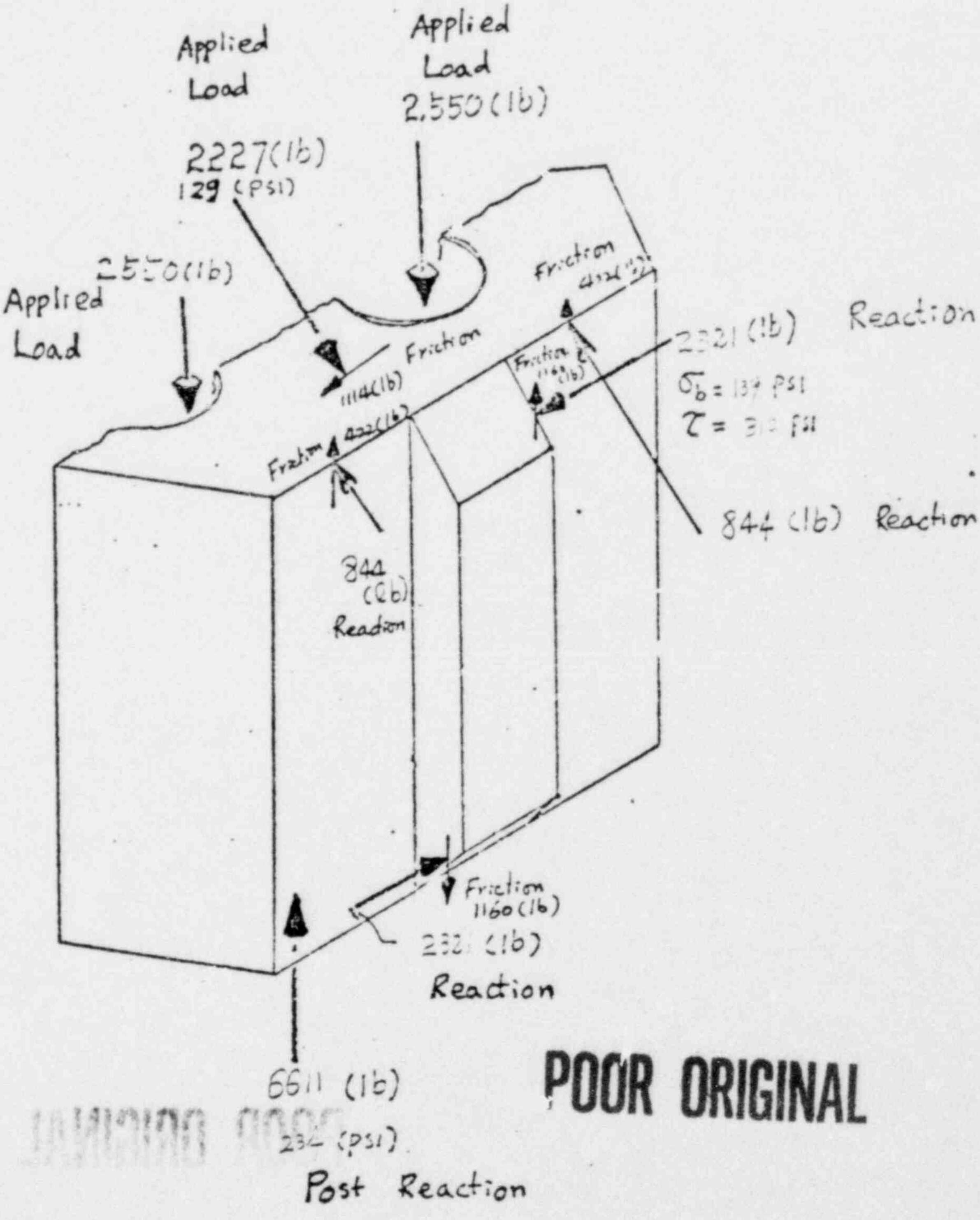

Fig. 13. Loads on cracked block with friction forces before key sheared off - case 2

5.2. STRESS RESULTS

Of significance to the accident scenario is the integrity of the CS post under each outer piece of the block and the integrity of the key which is holding the block in rotational equilibrium. It is also of interest to determine if the bearing stress between the center piece and each of the outer pieces at the cracked web surface is of any consequence.

The maximum stress anywhere in the block is found to be the tensile stress associated with shear force on the interblock keys. This maximum principal tensile stress is estimated to be 343 psi which is 30% of the minimum tensile strength of PGX.

It can be concluded from this analysis that the keys will not fail and the equilibrium position of the block pieces will be established by the keys jamming in their respective keyway. The amount of block rotation is less than 0.2° which is imperceptible with respect to fuel column tilting.

6. ANALYSIS OF CRACKED BLOCK - WITHOUT KEYS

An even more conservative step in the scenario is to assume that the cracked block keys shear off and do not provide rotational restraint to the outer pieces of the CS block even though the stress analysis showed the keys do not fail. Once the keys are sheared off, equilibrium can only be maintained by the pieces of the CS block rotating until they jam between the adjacent blocks as shown in Figs. 14 and 15. Only the case without friction-force is considered herein. This scenario could potentially result in a more serious disarray of the fuel columns.

6.1. FORCE EQUILIBRIUM

Results of forces on the CS block with the key sheared off are shown for the cracked block in Fig. 14. See Appendix F for the detailed calculations.

6.2. STRESS RESULTS

Stress results are identical with the results given in Table 2 except that the key stresses are not relevent to this scenario. The 2000-lb loads on opposite corners will cause some local crushing but do not result in any other significant stresses.

6.3. JAMMED CORE SUPPORT BLOCK

In this hypothetical scenario, the CS block piece rotates about the post due to the weight of the fuel columns until it contacts the side of an adjacent CS block near the top. Then it slides down until the opposite bottom corner touches the other adjacent CS block. These movements cause one side of the block to drop 1.4 in. as shown in Fig. 15. The angle of

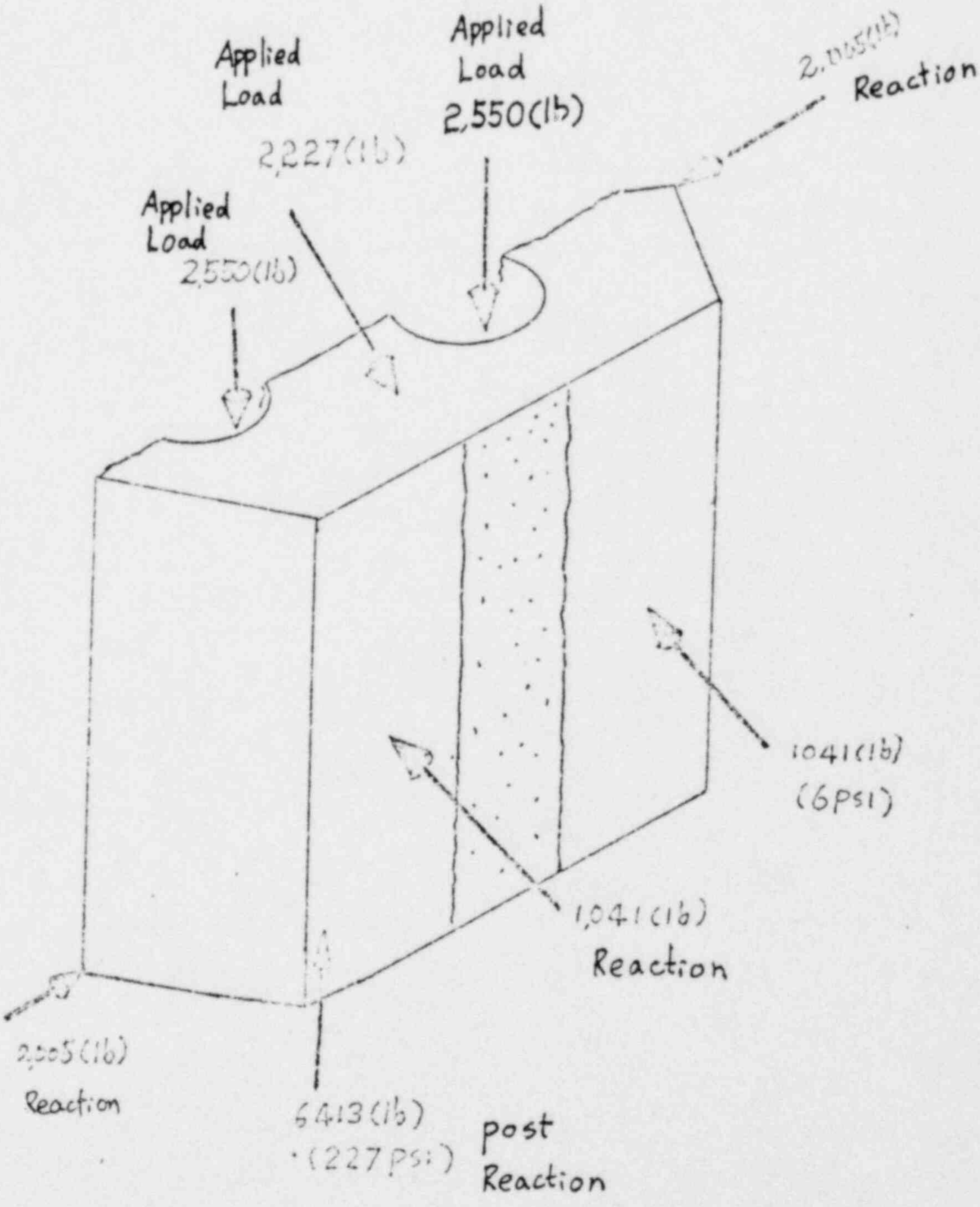

Fig. 14. Loads on block after key sheared off

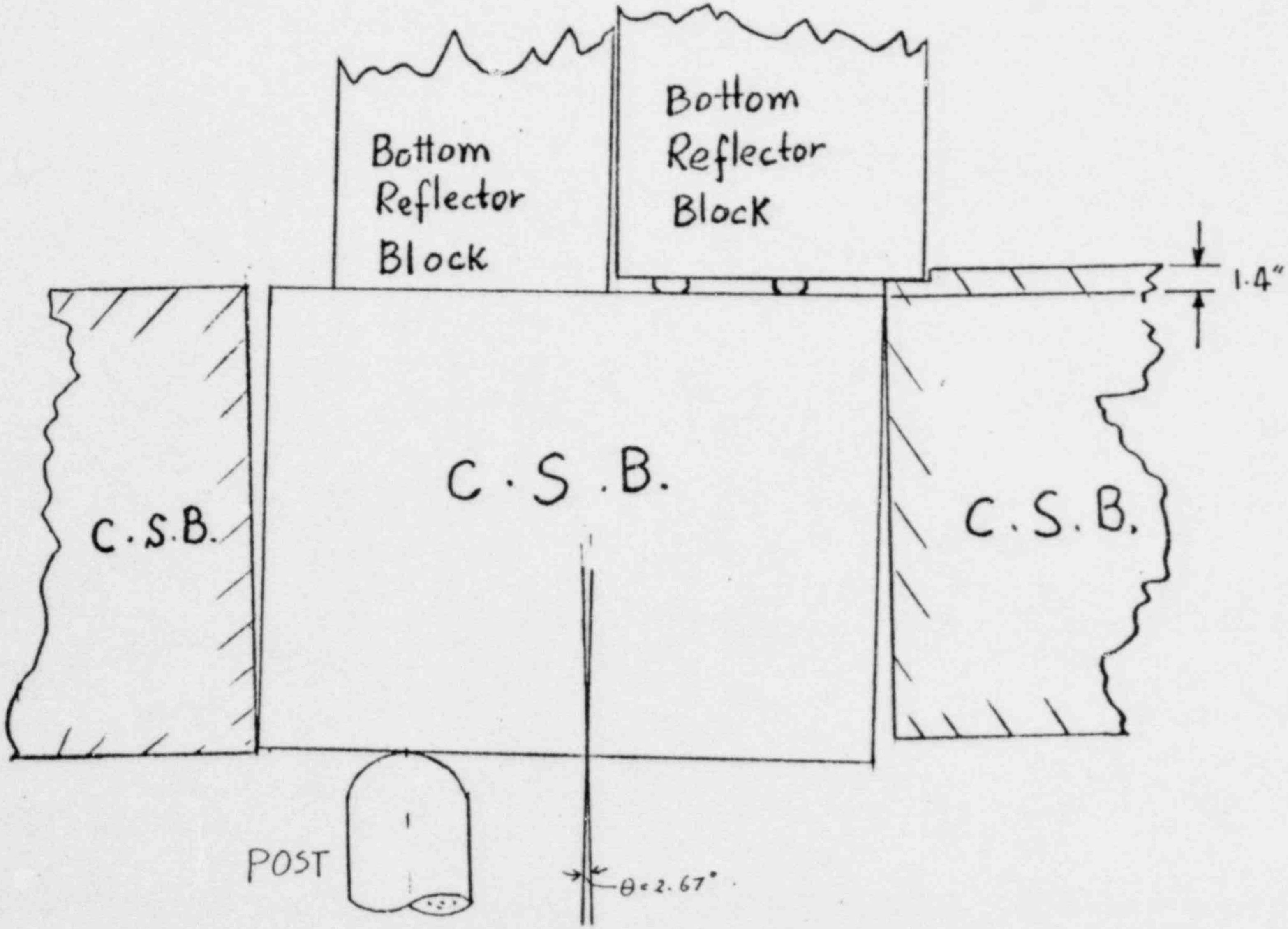

Fig. 15. Jammed core support block

TABLE 2
STRESS RESULTS (psi)

Minimum ultimate tensile strength of PGX graphite (Ref. 6)	1160
Minimum ultimate compressive strength of PGX graphite (Ref. 6)	4460
Minimum ultimate compressive strength of ATJ graphite (Ref. 6)	7204
Results from frictionless surface assumption	
Bearing stress on the slanted surface of web	129
Bearing stress on a flat surface	6
Maximum shear stress on a key	343
Maximum bending stress on a key	154
Compressive stress in a post (ATJ graphite)	227
Results from the consideration of friction forces on cracked CS block	
Bearing stress on a flat surface	4.4
Maximum shear stress on a key	310
Maximum bending stress on a key	139
Compressive stress in a post (ATJ graphite)	234

rotation of the block is 2.7°. Detailed calculation of these movements are contained in Appendix F.4.

It should be noted that the fuel column which overhangs the adjacent core support block on the dropped side is lifted and tilted radially inward. The fuel columns in this mode of tilt lean against the central fuel column of the region without "jawing" of the horizontal joints between blocks. The dowels pull free from the CS block.

At this point in the scenario the peripheral fuel columns are leaning against the central column much like a stack of rifles. The angles of tilt are less than 0.2°. Figure 16 is a scale drawing of the tilted CS block pieces and the bottom block in each fuel column. The central section has dropped down about 2.6 in. along with the central column. The disarray is difficult to see in this drawing because the movements are very small compared to the dimensions of the blocks and the height of the fuel columns.

The coolant flow through the fuel columns, whether it be upward or downward, is not inhibited by the cracked and tilted block. The large coolant holes in the bottom reflector blocks intersect the triangular shaped space in the center of the cracked block. This triangular-shaped block in turn intersects the large coolant channels in the CS block which communicate to the lower plenum. Thus, the flow path is changed, but, unimpaired.

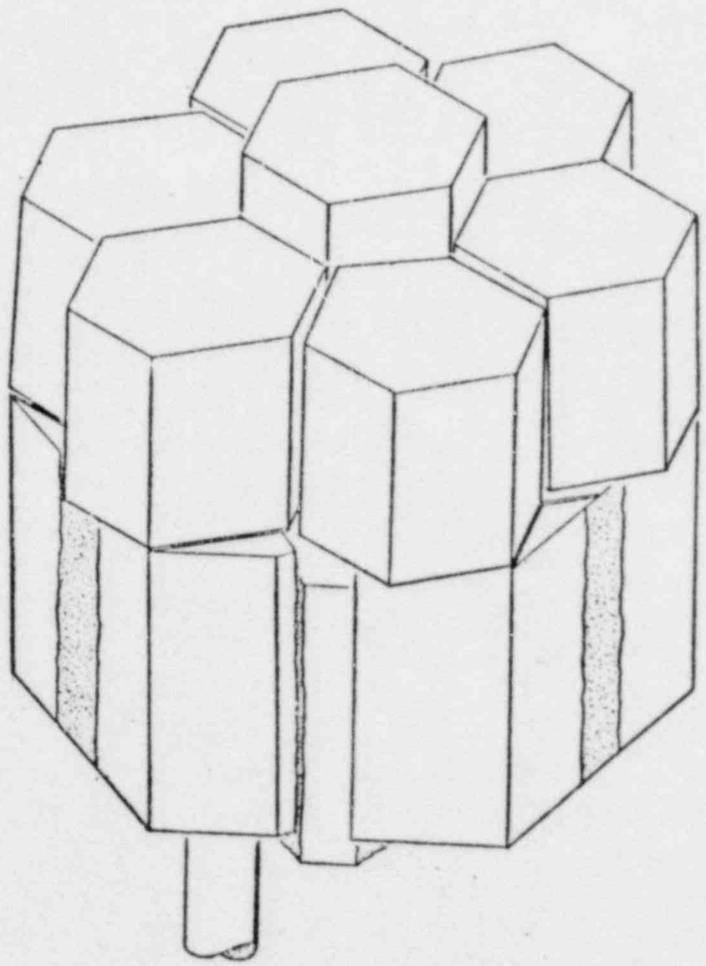

Fig. 16. Cracked and tilted core support block and bottom block of each fuel column in a region

7. SUMMARY OF RESULTS

The results of this analysis can be summarized as follows.

1. The extent of cracking assumed is extremely conservative, since the stresses calculated by LASL resulting from thermal gradients and are highly peaked in the corners of the keyways. Furthermore, cracks initiated in these corners are not expected to propagate through the block from top to bottom.

2. Gaps between blocks are assumed large, ince core barrel expansion determines these gaps. Th~ core barrel temperature was assumed to be 2300°F instead of about 1150°F to be conservative.

3. Core support block key stresses are low. Thus, the region disarray resulting from the "sheared key scenario" is considered to be an extreme.

4. Core support block pieces remain jammed between adjacent core support blocks. This precludes region collapse keeping significant amounts of debris from falling into the lower plenum.

5. Disarray of fuel blocks is minimal and occurs only at the core support floor/bottom reflector interface. Thus, coolant flow through the fuel blocks is unimpaired.

6. The core support block continues to function in the cracked condition.

8. CONCLUSION

From the results of this analysis it can be concluded that cracking of a core support block in the conservative manner assumed does not interfere with safe cooldown of the reactor core.

9. REFERENCES

1. "Fort St. Vrain Nuclear Generating Station Final Safety Analysis Report," Vol. I, 3.3.2.2.
2. Bradley, E., "Interim Report on Gap Comparison Study - Core Fluctuation Investigation," General Atomic Document No. 904658.
3. "Reactor Internals Assembly - FSV," General Atomic Drawing No. 90-SK-5523.
4. "FSV Nuclear Generating Station Final Safety Analysis Report," Vol. IV, Fig. D.1-23.
5. "FSV Nuclear Generating Station Final Safety Analysis Report," Vol. I, Table 3.1-1.
6. Salavatcioglu, R., "Generic - Graphite Design Material Properties," General Atomic Document No. 904434, pp.73 and 119.

10. ACKNOWLEDGMENT

The authors deeply wish to thank Dr. F. Ho for his independent review.

APPENDIX A

WEIGHT CALCULATION

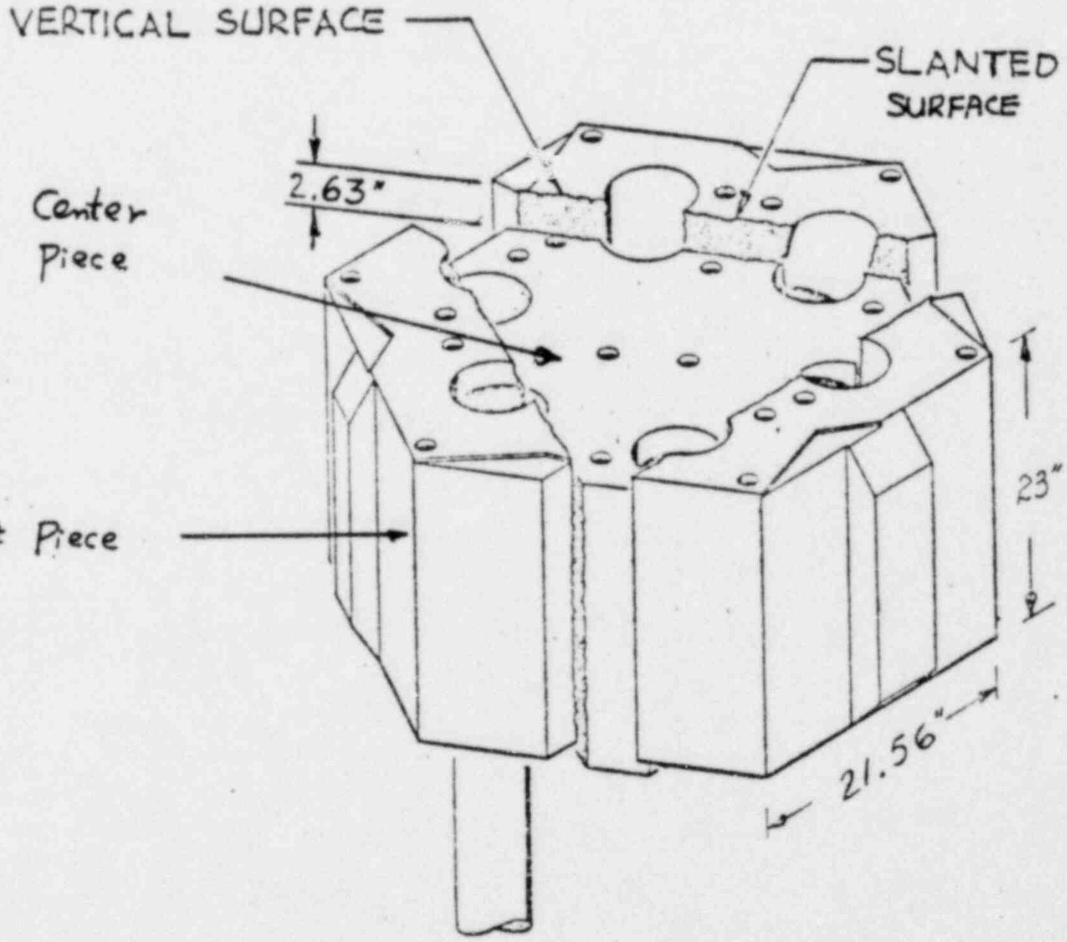

POOR ORIGINAL

Fig. 17. Dislocation of center piece of CSB

A.1. NET VOLUME OF CENTER PIECE

Approximate volume is only obtained in the following way:

$$\begin{aligned}\text{Net volume of center piece} = \ & \text{Volume *(opQLMN)} \\ & -3 \times [\text{Volume *}(ABJ'K'A'B')] \\ & -3 \times [\text{Volume of coolant channel}] \\ & -3 \times [\text{Volume *(LJSOGR)}]\end{aligned}$$

a. Volume *(opQLMN) $= \frac{1}{2}(35.84'' \times 35.84 \sin 60) \times 8''$
$= 4449.66 \approx 4450 \text{ in.}^3$

b. Volume *(ABJ´K´A´B´) $= \frac{1}{2}(18.05'' \times 3.03'') \times 8''$
$\cong 265 \text{ in.}^3$

c. Volume of Coolant Channel $= \pi \times (4.037'' \times 3.775) \times 8''$
$\simeq 373 \text{ in.}^3$

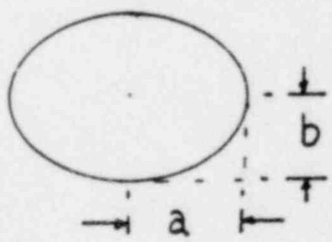

$b = 3.775''$

Area $= \pi ab$

$a = 3.775/\cos 20.75°$

d. Volume *(LJSOGR) $= \frac{1}{2}(5.062 \times 5.062 \sin 60) \times 8''$
$= 88.76 \text{ in.}^3$

∴ Net volume of center piece

$= a - 3b - 3c - 3d$
$= 2378.05 \text{ in.}^3$

---

*See Fig. 18.

A.2. WEIGHT OF CENTER PIECE

Weight of center piece is obtained as follows:

$$Wc = \delta \times Vc$$

where δ = weight density of PGX graphite,
= 0.064 lb/in.^{3},
Vc = volume of center piece,
Wc = weight of center piece.

$$Wc = 0.064 \text{ lb/in.}^3 \times 2378.05 \text{ in.}^3$$
$$Wc = 152 \text{ lbf}$$

A.3. WEIGHT OF POST PIECE

Weight of each post piece:

$$= \frac{\text{Weight of CSB - Weight of Center Piece}}{3}$$

$$= (1723^* - 152)/3 = 523.6 \text{ lbf}$$

---

*Obtained from the following way.
$(21.56" \times \cos 30°) \times 21.56" \times 3 \times 23"$
$-(\pi\ 7.55^2/4) \times 6 \times 8"/\cos 20.45°$
$-(\pi\ 21^2/4) \times 15"$ - seats etc.
=220.00 in.^{3}
=12.73 ft^3
12.73 x 110 lb/ft^3 = 1400 lb

a. Core weight including CSB = 19.238 lb (Ref. 8)
b. Weight of core excluding CSB =

Wt of 6 fuel columns + Wt of control rod column
(6 x 2550 lb) (2515 lb) (Ref. 9)
= 17,515 lb
∴ a-b = 19,238 - 17,515 = 1723 lb

APPENDIX B

KINEMATICS OF CSB

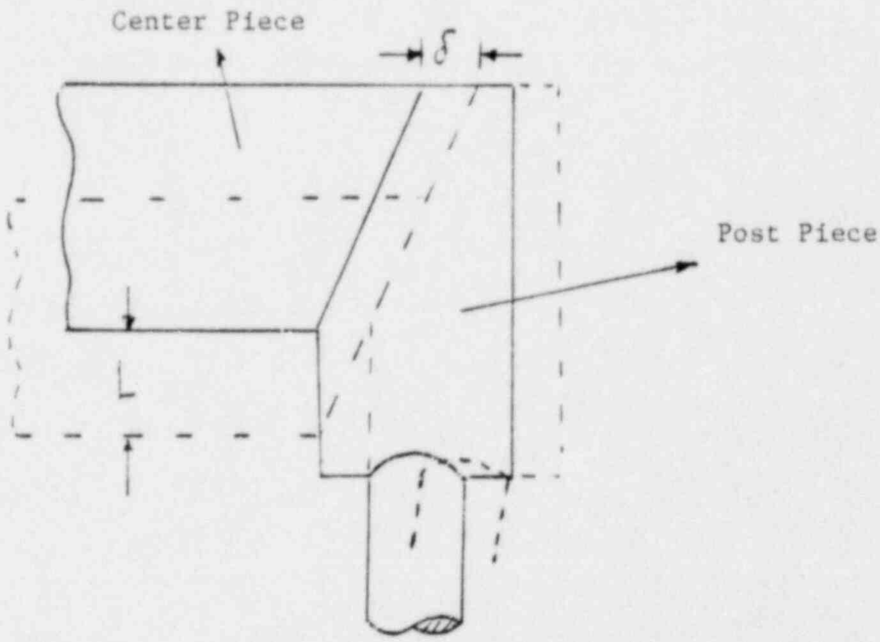

where δ = radial displacement by P-Piece,

= 1.0 in. (calculated in Appendix G.2),

L = vertical displacement by center piece,

$L = \delta/\tan 20.75°$,

$= 1\text{ in.}/\tan 20.75° = 2.63\text{ in.}$

POOR ORIGINAL

APPENDIX C

BEARING SURFACE AREA

Each bearing surface between center and post piece is approximately shown below.

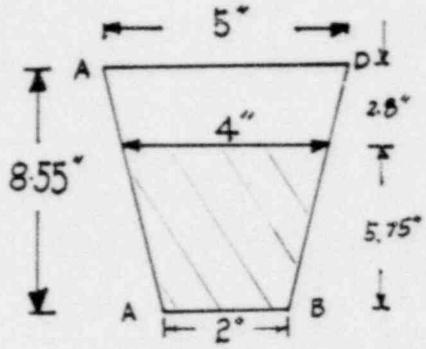

From Fig. 16

Bearing Surface Area $= \frac{1}{2}(4 + 2)\ 5.75 = 17.25$

$= 17.25\ \text{in.}^2$

POOR ORIGINAL

APPENDIX D

STATIC EQUILIBRIUM OF CENTER PIECE OF CSB

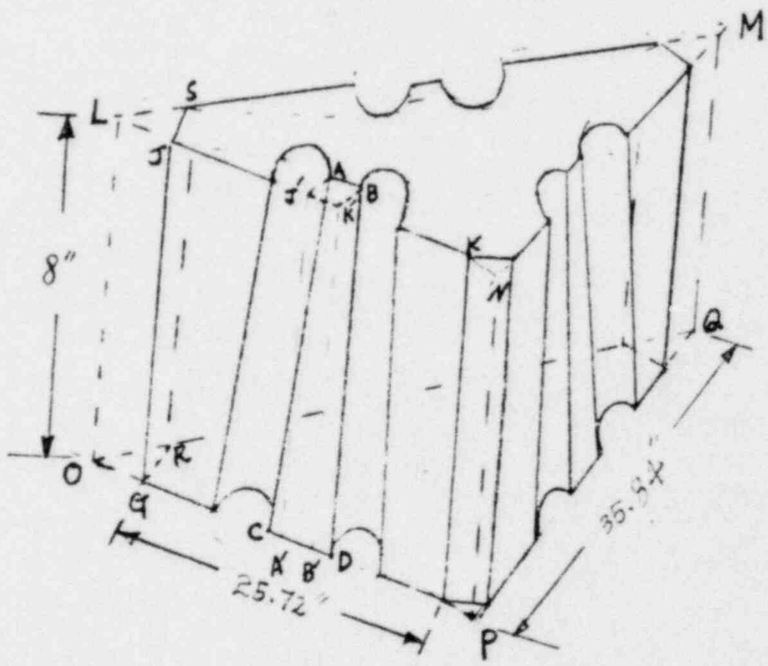

Fig. 18. A part of center piece of CSB (upside down)

Assumption:

Magnitudes of reaction forces acting normal to slanted surfaces are identical.

D.1. FORCE ON SLANTED SURFACE

W = Weight of control element column and center piece

Weight of control element column = 2,215 lbf

Weight of center piece = 152 lbf

$W = 2,215 + 152 = 2,367$ lbf.

$\underset{\sim}{R}_i$ = Reaction force resultants acting on slanted surfaces.
$(i = 1 \text{ to } 3)$

so

$$|\underset{\sim}{R}_1| = |\underset{\sim}{R}_2| = |\underset{\sim}{R}_3| = R_c$$

$$R_{cy} = \frac{W}{3} = R_c \cos 69.25°$$

$$R_c = (\frac{1}{3} W)/\cos 69.25°$$

$$= 2227 \text{ lbf}$$

D.2. BEARING STRESS ON SLANTED SURFACE

Assuming uniformly distributed

$$\text{Bearing stress} = 2227 \text{ lbf}/17.25 \text{ in.}^2$$

$$= 129.1 \text{ psi}$$

Maximum bear stress may be higher by a factor of 2 or 3, due to non-uniform distribution, say 350 psi maximum.

APPENDIX E

ANALYSIS OF CRACKED BLOCK - WITH KEYS

E.1. FORCE EQUILIBRIUM

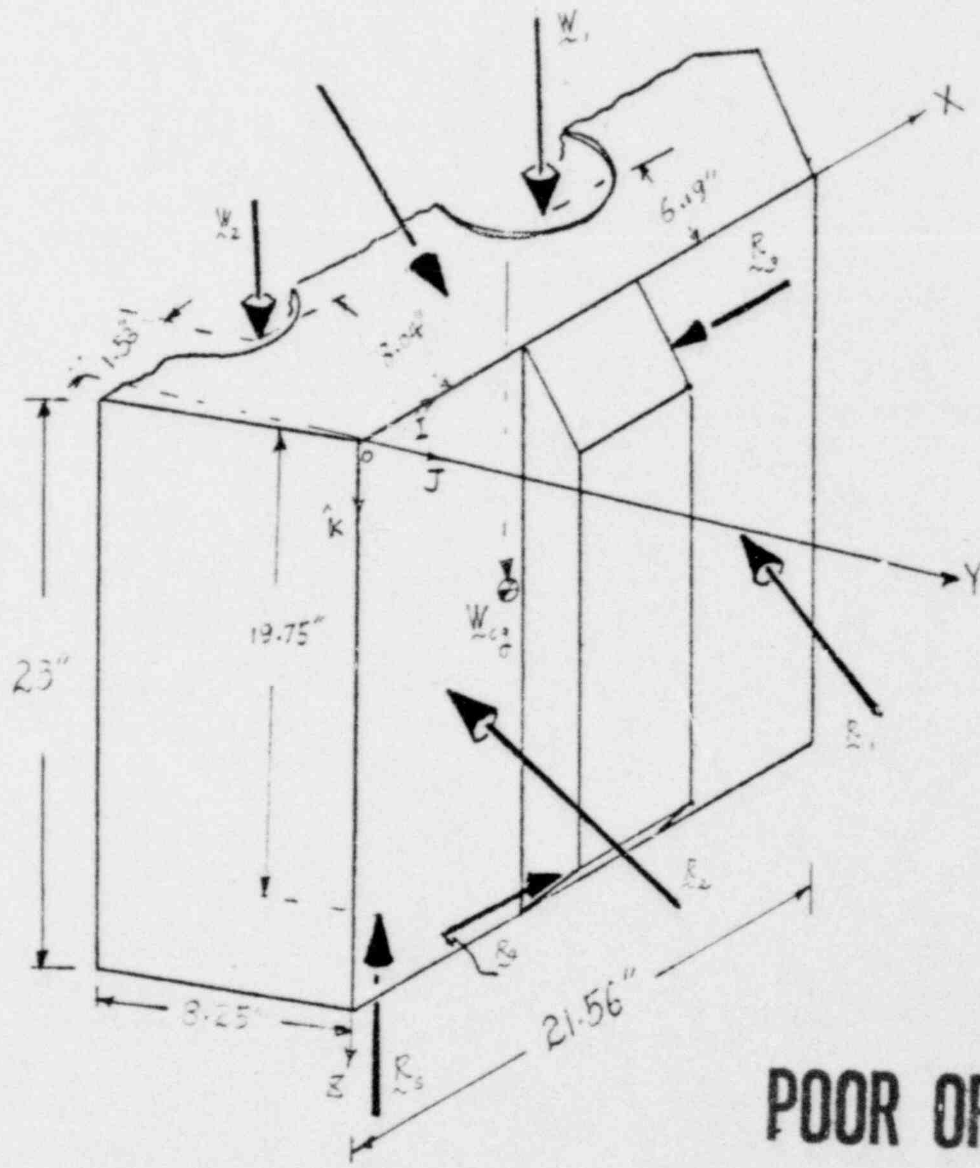

Fig. 19. Force equilibrium without friction forces

Nomenclature

a. Forces

$\underset{\sim}{W}_{cg}$ = Weight of post piece

$\underset{\sim}{W}_1$, $\underset{\sim}{W}_2$ = Weight of standard fuel column

$\underset{\sim}{R}_3$ and $\underset{\sim}{R}_4$ = Reaction forces acting on top and bottom key respectively

$\underset{\sim}{R}_1$ and $\underset{\sim}{R}_2$ = Reaction forces acting on a flat face of post piece

$\underset{\sim}{R}_s$ = Reaction force by post

$\underset{\sim}{R}_c$ = Reaction force normal to the slanted surface.

b. Distance Vector

$\underset{\sim}{\gamma}_{cg}$ = Distance vector from the origin 0 to where W_{cg} is acting

$\underset{\sim}{\gamma}_{W1}$ and $\underset{\sim}{\gamma}_{W2}$ = Distance vectors from the origin 0 to where W_1 and W_2 are acting

$\underset{\sim}{\gamma}_3$ and $\underset{\sim}{\gamma}_4$ = Distance vectors from the origin 0 to where R_3 and R_4 are acting

$\underset{\sim}{\gamma}_1$ and $\underset{\sim}{\gamma}_2$ = Distance vectors from the origin 0 to where R_1 and R_2 are acting

$\underset{\sim}{\gamma}_s$ = Distance vector from the origin 0 to where R_s is acting

$\underset{\sim}{\gamma}_c$ = Distance vector from the origin 0 to where R_c is acting

(1) $\underset{\sim}{\gamma}_{cg} = 10.78\hat{I} - 402\hat{J} + 11.5\hat{K}$

$\underset{\sim}{W}_{cg} = 523.6\hat{K}$

$$\underset{\sim}{M}_o = \underset{\sim}{\gamma}_{cg} \times \underset{\sim}{W}_{cg}$$
$$= -2104.87\hat{I} - 5644.41\hat{J}$$

(2) $\underset{\sim}{\gamma}_{W1} = 16.21\hat{I} - 6.19\hat{J}$

$\underset{\sim}{W}_1 = 2550\hat{K}$

$\underset{\sim}{M}_o = \underset{\sim}{\gamma}_{W1} \times \underset{\sim}{W}_1 = -15784.5\hat{I} - 41335.5\hat{J}$

(3) $\underset{\sim}{\gamma}_{W2} = 1.53\hat{I} - 8.04\hat{J}$

$\underset{\sim}{W}_2 = 2550\hat{K}$

$\underset{\sim}{M}_o = \underset{\sim}{\gamma}_{W2} \times \underset{\sim}{W}_2$

$= -20502\hat{I} - 3901.5\hat{J}$

(4) $\underset{\sim}{\gamma}_3 = 13.28\hat{I} + 1.125\hat{J} + 3.2\hat{K}$

$\underset{\sim}{R}_3 = -R_3\hat{I}$

$\underset{\sim}{M}_o = \underset{\sim}{\gamma}_3 \times \underset{\sim}{R}_3 = -3.2\ (R_3)\hat{J} + 1.125\ (R_3)\hat{K}$

(5) $\underset{\sim}{\gamma}_4 = 8.28\hat{I} + 1.125\hat{J} + 19.8\hat{K}$

$\underset{\sim}{R}_4 = R_4\hat{I}$

$= 19.8\ (R_4)\hat{J} - 1.125\ (R_4)\hat{K}$

(6) $\underset{\sim}{\gamma}_1 = 17.41\hat{I} + 11.5\hat{K}$

$\underset{\sim}{R}_1 = -R_1\hat{J}$

$\underset{\sim}{M}_o = \underset{\sim}{\gamma}_1 \times \underset{\sim}{R}_1$

$= 11.5\ (R_1)\hat{I} - 17.42\ (R_1)\hat{K}$

Not necessary at the centroid of the face (near top) (no friction force)

(7) $\underset{\sim}{\gamma}_2 = 4.13\hat{I} + 11.5\hat{K}$

$\underset{\sim}{R}_2 = -R_2\hat{J}$

$$\underset{\sim}{M}_o = \underset{\sim}{\gamma}_2 \times \underset{\sim}{R}_2$$

$$= 11.5\ (R_2)\hat{I} - 4.14\ (R_2)\hat{K}$$

(8) $\underset{\sim}{\gamma}_s = 2.6\hat{I} - 4.5\hat{J} + 19.75\hat{K}$

$$\underset{\sim}{R}_s = -R_s\hat{K}$$

$$\underset{\sim}{M}_o = \underset{\sim}{\gamma}_s \times \underset{\sim}{R}_s$$

$$= 4.5\ (R_s)\hat{I} + 2.6\ (R_s)\hat{J}$$

(9) $\underset{\sim}{\gamma}_c = 10.78\hat{I} - \gamma_c\hat{J} + 3.11\hat{K}$

$$\underset{\sim}{R}_c = 2227\ (\cos 20.75\hat{J} + \sin 20.75\hat{K})$$

$$\underset{\sim}{M}_o = \underset{\sim}{\gamma}_c \times \underset{\sim}{R}_c$$

$$= (-789\ \gamma_c - 6{,}476.7)\hat{I} - 8{,}505.53\hat{J}$$

$$+ 22{,}450\hat{K}$$

TABLE 3
SUMMARY OF STATIC EQUILIBRIUM ANALYSIS - WITH KEYS

	Distance Vector (in.)			Force Vector (lbf)			Moment Vector (in.-lbf) (Distance Vector x Force Vector)		
	$\hat{I}$	$\hat{J}$	$\hat{K}$	$\hat{I}$	$\hat{J}$	$\hat{K}$	$\hat{I}$	$\hat{J}$	$\hat{K}$
1	10.78	-4.02	11.5	0	0	523.6	-2,104.87	-5,644.41	0
2	16.21	-6.19	0	0	0	2,550	-15,784.5	-41,335.5	0
3	1.54	-8.04	0	0	0	2,550	-20,502	-3,901.5	0
4	13.28	1.125	3.2	$-R_3$	0	0	0	$-3.2\ (R_3)$	$1.125\ (R_3)$
5	8.28	1.125	19.8	R_4	0	0	0	$19.8\ (R_4)$	$-1.125\ (R_4)$
6	17.42	0	11.5	0	$-R_1$	0	$11.5\ (R_1)$	0	$-17.42\ (R_1)$
7	4.14	0	11.5	0	$-R_2$	0	$11.5\ (R_2)$	0	$-4.14\ (R_2)$
8	2.6	-4.5	19.75	0	0	$-R_s$	$4.5\ (R_s)$	$2.6\ (R_s)$	0
9	10.78	$-\gamma_c$	3.11	0	2,082.55	789.01	$-789\gamma_c - 6,476.7$	-8,505.53	22,450

$\Sigma F_x = 0 \qquad \Sigma Mo_x = 0 \qquad R_1 = R_2 = 1,041.27$ lbf $\qquad \underline{\gamma}_c = 10.78\hat{I} - 10.06\hat{J} + 3.11\hat{K}$

$\Sigma F_y = 0 \qquad \Sigma Mo_y = 0 \qquad R_3 = R_4 = 2,573.14$ lbf

$\Sigma F_z = 0 \qquad \Sigma Mo_z = 0 \qquad \underline{R}_s = -6412.6\hat{K}$ (lbf)

E.1.1. Force Equilibrium Considering Friction Forces - Case 1

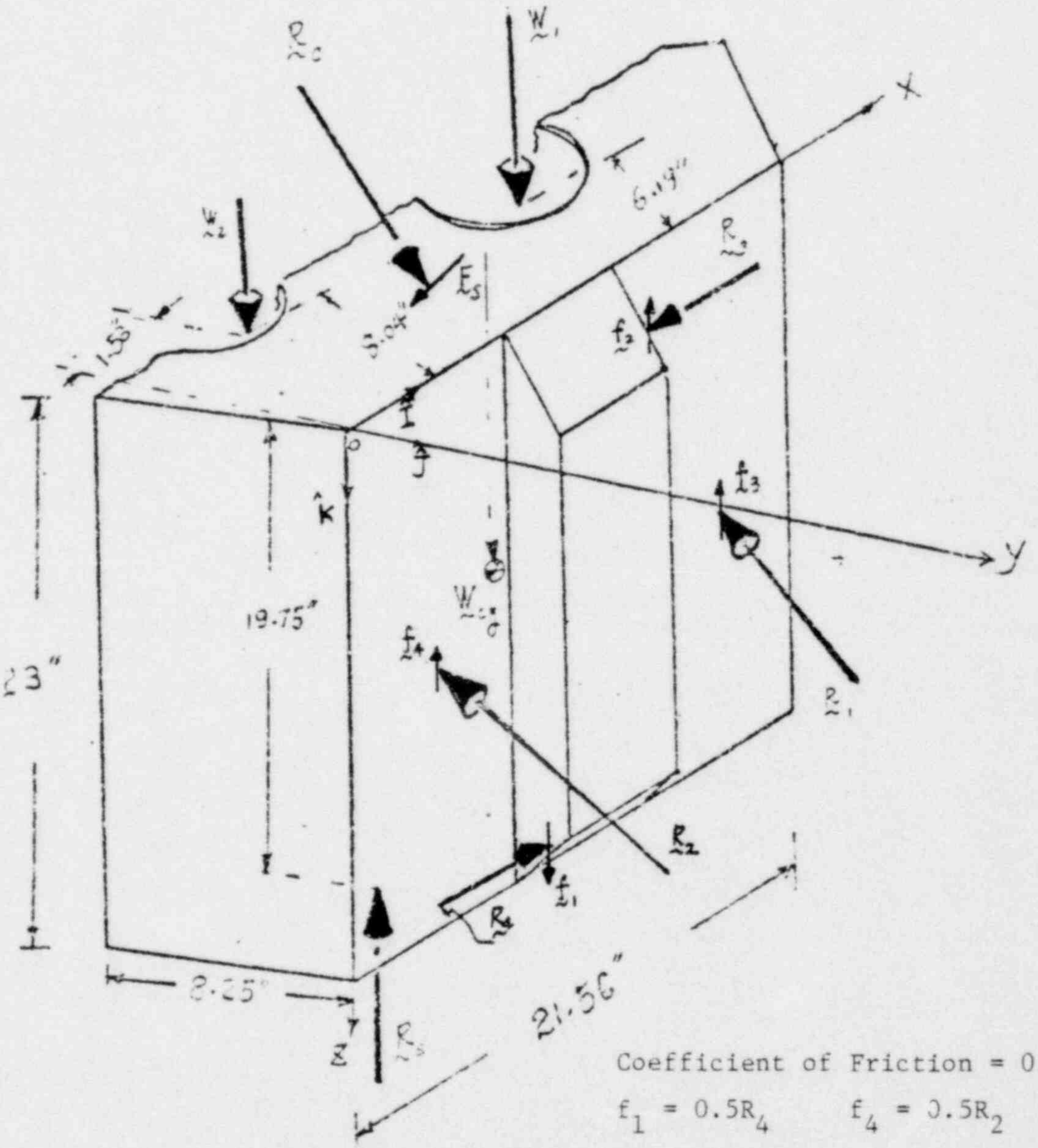

Coefficient of Friction = 0.5

$f_1 = 0.5R_4$ $\quad$ $f_4 = 0.5R_2$

$f_2 = 0.5R_3$ $\quad$ $f_5 = 0.5R_c$

$f_3 = 0.5R_1$

POOR ORIGINAL

Fig. 20. Force equilibrium with friction forces - case 1

TABLE 4

SUMMARY OF STATIC EQUILIBRIUM ANALYSIS WITH FRICTION FORCES - WITH KEYS, CASE 1

	Distance Vector (in.)			Force Vector (lbf)			Moment Vector (in.-lbf)		
	$\hat{I}$ (x)	$\hat{J}$ (y)	$\hat{K}$ (z)	$\hat{I}$ (x)	$\hat{J}$ (y)	$\hat{K}$ (z)	$\hat{I}$ (x)	$\hat{J}$ (y)	$\hat{K}$ (z)
1	10.78	-4.02	11.5	0	0	523.6	-2,104.87	-5,644.41	0
2	16.21	-6.19	0	0	0	2,550	-15,784.5	-41,335.5	0
3	1.54	-8.04	0	0	0	2,550	-20,502	-3,901.5	0
4	13.28	1.125	3.2	$-R_3$	0	0	0	$-3.2\ R_3$	$1.125\ R_3$
5	8.28	1.125	19.8	R_4	0	0	0	$19.8\ R_4$	$-1.125\ R_4$
6	17.42	0	11.5	0	$-R_1$	0	$11.5\ R_1$	0	$-17.42\ R_1$
7	4.14	C	11.5	0	$-R_2$	0	$11.5\ R_2$	0	$-4.14\ R_2$
8	2.6	-4.5	19.75	0	0	$-R_s$	$4.5\ R_s$	$2.6\ R_s$	0
9	10.78	$-\gamma_c$	3.11	0	2,082.5	789.01	$-789\ \gamma_c - 6,476.7$	-8,505.5	22,450
10	17.41	0	11.5	0	0	$-0.5\ R_1$	0	$8.71\ R_1$	0
11	4.13	0	11.5	0	0	$-0.5\ R_2$	0	$2.06\ R_2$	0
12	8.28	1.125	19.8	0	0	$0.5\ R_4$	$0.56\ R_4$	$-4.14\ R_4$	0
13	13.28	1.125	3.2	0	0	$-0.5\ R_3$	$-0.56\ R_3$	$6.64\ R_3$	0
14	10.78	$-\gamma_c$	3.11	0	-395	1.042	$-1,042\ \gamma_c + 1,228.45$	-11,232.76	-4,258.1

$\Sigma \underset{\sim}{F}_x = 0 \qquad R_3 = R_4 \qquad \Sigma \underset{\sim}{M}o_z = 0 \qquad R_1 = R_2 = 844$

$\Sigma \underset{\sim}{F}_y = 0 \qquad R_1 + R_2 = 1687.55 \qquad \Sigma \underset{\sim}{M}o_y = 0 \qquad R_3 = R_4 = 2321$

$\Sigma \underset{\sim}{F}_z = 0 \qquad R_s = 6611$

E.1.2. Force Equilibrium Considering Friction Forces - Case 2

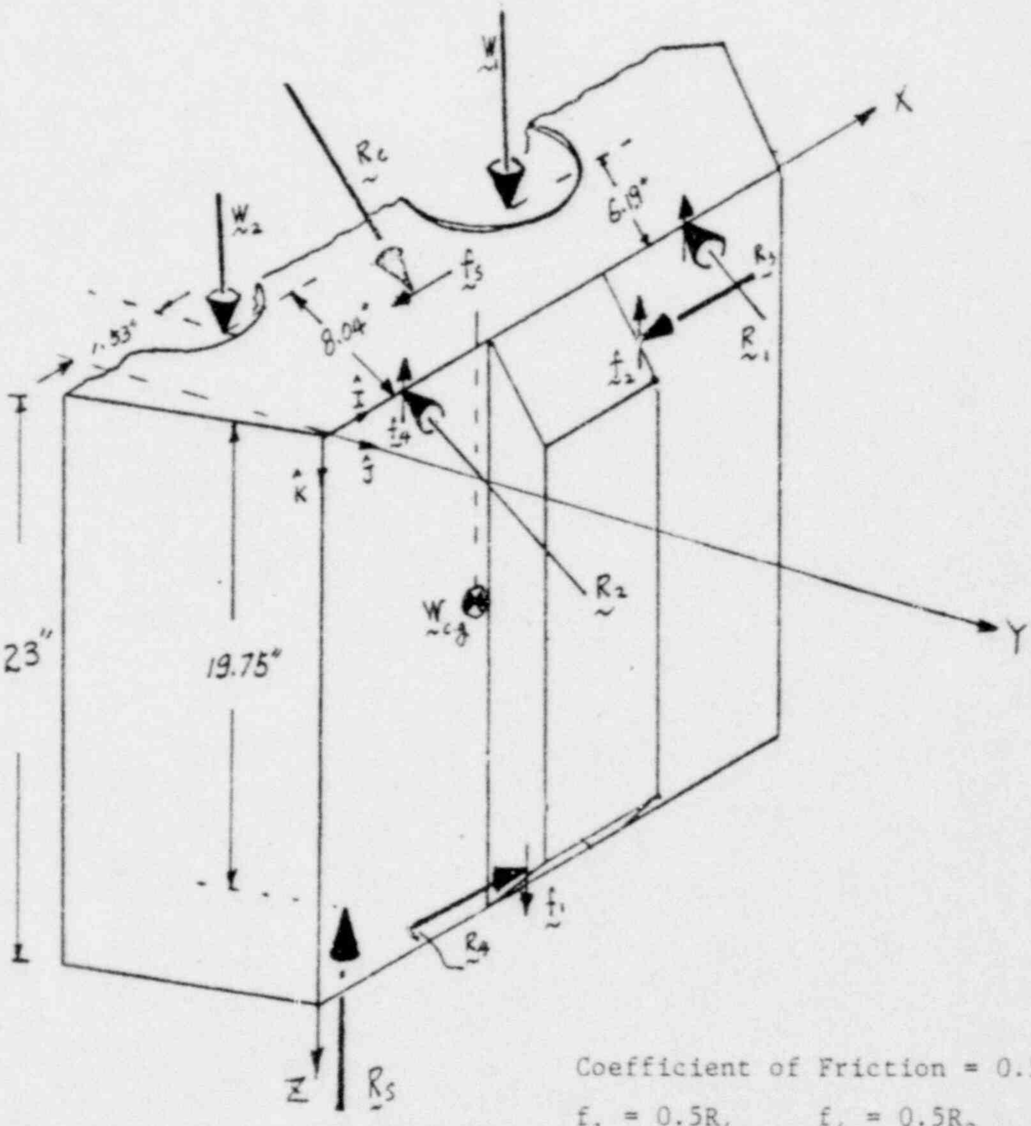

Coefficient of Friction = 0.5

$f_1 = 0.5R_4$ $\quad$ $f_4 = 0.5R_2$

$f_2 = 0.5R_3$ $\quad$ $f_5 = 0.5R_c$

$f_3 = 0.5R_1$

POOR ORIGINAL

Fig. 21. Force equilibrium with friction forces - case 2

TABLE 5

SUMMARY OF STATIC EQUILIBRIUM ANALYSIS WITH FRICTION FORCES - WITH KEYS, CASE 2

	Distance Vector (in.)			Force Vector (lbf)			Moment Vector (in.-lbf)		
	$\hat{I}$ (x)	$\hat{J}$ (y)	$\hat{K}$ (z)	$\hat{I}$ (x)	$\hat{J}$ (y)	$\hat{K}$ (z)	$\hat{I}$ (x)	$\hat{J}$ (y)	$\hat{K}$ (z)
1	10.78	-4.02	11.5	0	0	523.6	-2,104.87	-5,644.4	0
2	16.21	-6.19	0	0	0	2,550	-15,784.5	-41,335.5	0
3	1.53	-8.04	0	0	0	2,550	-20,502	-3,901.5	0
4	8.28	1.125	19.8	R_4	0	0	0	19.8 R_4	-1.125 R_4
5	13.28	1.125	3.2	$-R_3$	0	0	0	-3.2 (R_3)	1.125 R_3
6	17.41	0	0	0	$-R_1$	0	0	0	-17.42 R_1
7	4.13	0	0	0	$-R_2$	0	0	0	-4.13 R_2
8	17.41	0	0	0	0	-0.5 R_1	0	8.71 R_1	0
9	4.13	0	0	0	0	-0.5 R_2	0	2.07 R_2	0
10	8.28	1.125	19.8	0	0	0.5 R_4	0.56 R_4	-4.14 R_4	0
11	13.28	1.125	3.2	0	0	-0.5 R_3	-0.56 R_3	6.64 R_3	0
12	2.6	-4.5	19.75	0	0	$-R_s$	4.5 (R_s)	2.6 (R_s)	0
13	10.78	$-Y_c$	3.11	0	2,082.55	789	-789 Y_c - 6,476.7	-8,505.5	22,450
14	10.78	$-Y_c$	3.11	0	-395	1,042	1,228 - 1,1042 Y_c	-11,233	-4,258.1

$\Sigma \underset{\sim}{F}_x = 0$ $R_3 = R_4$ $\Sigma \underset{\sim}{Mo}_z = 0$ $R_1 = R_2 = 844$

$\Sigma \underset{\sim}{F}_y = 0$ $R_1 + R_2 = 1,687.55$ $\Sigma \underset{\sim}{Mo}_y = 0$ $R_3 = R_4 = 2,321$

$\Sigma \underset{\sim}{F}_z = 0$ $R_s = 6,611$

E.2. STRESS RESULTS

E.2.1. Shear Stress On a Key

To be conservative, shear force transmits through area (= 5" x 2.25")

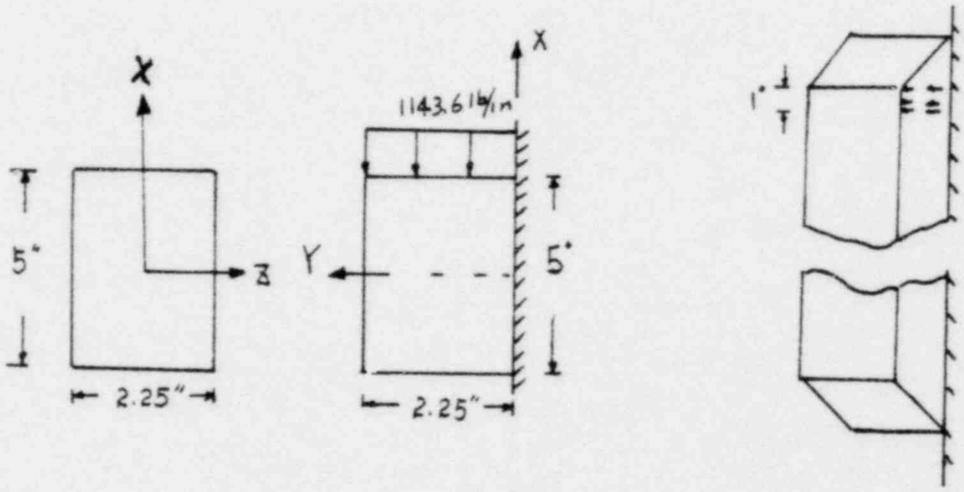

Maximum Shear Stress

a) $\tau_{max} = \frac{V_{(max)}}{A}(\frac{3}{2}) = \frac{2573}{(5" \times 2.25")}(\frac{3}{2}) = 343$ (psi)
(w/o friction)

b) $\tau_{max} = \frac{2321}{(5" \times 2.25")}(\frac{3}{2}) = 310$ (psi) with friction forces

E.2.2. Maximum Bending Stress On a Key

$$\sigma_{max} = \frac{1143.6 \times (\frac{2.25}{2}) \times 2.5}{\frac{1}{12}(2")\ 5^3} = 154 \text{ psi}$$

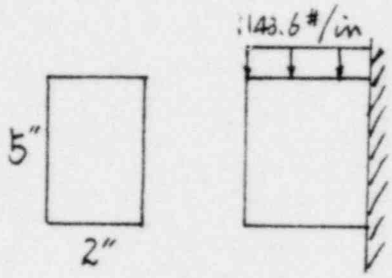

Considering a stress concentration factor = 2

$\sigma = 2 \cdot \sigma_{max}$ = 308 psi (w/o friction)

$\sigma = 2 \cdot \sigma_{max}$ = 279 psi (w/friction)

APPENDIX F

ANALYSIS OF CRACKED BLOCK - WITHOUT KEYS

F.1. FORCE EQUILIBRIUM

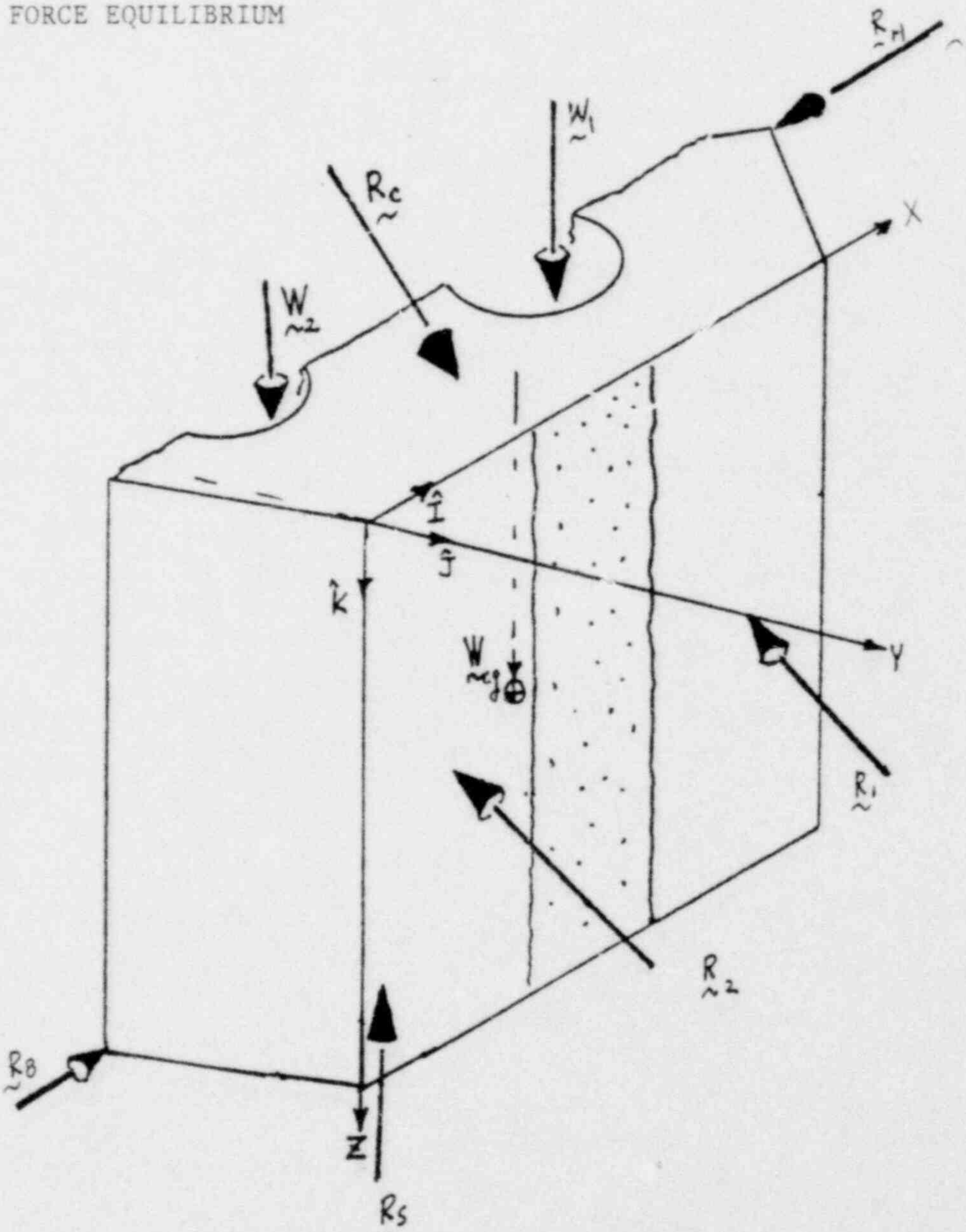

POOR ORIGINAL

$$(1)\quad \underset{\sim}{\gamma}_{cg} = 10.78\hat{I} - 4.02\hat{J} + 11.5\hat{K}$$

$$\underset{\sim}{W}_{cg} = 523.6\hat{K}$$

$$\underset{\sim}{M}_{o} = \underset{\sim}{\gamma}_{cg} \times \underset{\sim}{W}_{cg}$$

$$= -2104.87\hat{I} - 5644.4\hat{J}$$

$$(2)\quad \underset{\sim}{\gamma}_{w1} = 16.21\hat{I} - 6.19\hat{J}$$

$$\underset{\sim}{W}_{1} = 2550\hat{K}$$

$$\underset{\sim}{M}_{o} = \underset{\sim}{\gamma}_{w1} \times \underset{\sim}{W}_{1}$$

$$= -15784.5\hat{I} - 41335.5\hat{J}$$

$$(3)\quad \underset{\sim}{\gamma}_{w2} = 1.53\hat{I} - 8.04\hat{J}$$

$$\underset{\sim}{W}_{2} = 2550\hat{K}$$

$$\underset{\sim}{M}_{o} = \underset{\sim}{\gamma}_{2} \times \underset{\sim}{W}_{2} = -20502\hat{I} - 3901.5\hat{J}$$

$$(4)\quad \underset{\sim}{\gamma}_{H} = 25.64\hat{I} - 7.17\hat{J} + 1.4\hat{K}$$

$$\underset{\sim}{R}_{H} = -R_{H}\hat{I}$$

$$\underset{\sim}{M}_{o} = \underset{\sim}{\gamma}_{H} \times \underset{\sim}{R}_{H}$$

$$= -R_{H}\,(1.4\hat{J} + 7.17\hat{K})$$

$$(5)\quad \underset{\sim}{\gamma}_{B} = -4.74\hat{I} - 7.17\hat{J} + 22.7\hat{K}$$

$$\underset{\sim}{R}_{B} = R_{B}\hat{I}$$

$$\underset{\sim}{M}_{o} = \gamma_{B} \times \underset{\sim}{R}_{B}$$

$$= R_{B}\,(22.7\hat{J} + 7.17\hat{K})$$

$$(6)\quad \underset{\sim}{\gamma}_{1} = 17.42\hat{I} + 11.5\hat{K}$$

$$\underset{\sim}{R}_{1} = -R_{1}\hat{J}$$

$$\underset{\sim}{M}_{o} = \underset{\sim}{\gamma}_{1} \times \underset{\sim}{R}_{1}$$

$$= R_{1}\,(11.5\hat{I} - 17.42\hat{K})$$

(7) $\underset{\sim}{\gamma}_2 = 4.14\hat{I} + 11.5\hat{K}$

$\underset{\sim}{R}_2 = -R_2\hat{J}$

$\underset{\sim}{M}_o = \underset{\sim}{\gamma}_2 \times \underset{\sim}{R}_2$

$= R_2\ (11.5\hat{I} - 4.14\hat{K})$

(8) $\underset{\sim}{\gamma}_s = 2.6\hat{I} - 4.5\hat{J} + 19.75\hat{K}$

$\underset{\sim}{R}_s = -R_s\hat{K}$

$\underset{\sim}{M}_o = \underset{\sim}{\gamma}_s \times \underset{\sim}{R}_s$

$= R_s\ (4.5\hat{I} + 2.6\hat{J})$

(9) $\underset{\sim}{\gamma}_c = 10.78\hat{I} - \gamma_c\hat{J} + 3.11\hat{K}$

$\underset{\sim}{R}_c = 2082.5\hat{J} + 789\hat{K}$

$\underset{\sim}{M}_o = \underset{\sim}{\gamma}_c \times \underset{\sim}{R}_c$

$= (-789\ \gamma_c - 6476.7)\hat{I} - 8505.5\hat{J}$

$+ 22450\hat{K}$

F.2. BEARING STRESS ON A FLAT FACE

$\sigma_{\text{(without friction)}} = 1041\ \text{lb}/190\ \text{in.}^2 \approx 5.5 \approx 6\ \text{psi (average)}$

$\sigma_{\text{(with friction)}} = 844\ \text{lb}/190\ \text{in.}^2 \approx 4.4\ \text{psi}$

TABLE 6

SUMMARY OF STATIC EQUILIBRIUM ANALYSIS - WITHOUT KEYS

	Distance Vector (in.)			Force Vector (lbf)			Moment Vector (in.-lbf) (Distance Vector x Force Vector)		
	$\hat{I}$	$\hat{J}$	$\hat{K}$	$\hat{I}$	$\hat{J}$	$\hat{K}$	$\hat{I}$	$\hat{J}$	$\hat{K}$
1	10.78	-4.02	11.5	0	0	523.6	-2,104.87	-5,644.41	0
2	16.21	-6.19	0	0	0	2,550	-15,784.5	-41,335.5	0
3	1.53	-8.04	0	0	0	2,550	-20,502	-3,901.5	0
4	25.64	-7.17	1.4	$-R_4$	0	0	0	$-1.4\ R_4$	$-7.17\ R_H$
5	-4.74	-7.17	22.7	R_B	0	0	0	$22.7\ R_B$	$7.17\ R_B$
6	17.42	0	11.5	0	$-R_1$	0	$11.5\ R_1$	0	$-17.42\ R_1$
7	4.14	0	11.5	0	$-R_2$	0	$11.5\ R_2$	0	$-4.14\ R_2$
8	2.6	-4.5	19.75	0	0	$-R_s$	$4.5\ R_s$	$2.6\ R_s$	0
9	10.78	$-\gamma_c$	3.11	0	2,082.5	789	$-789\gamma_c - 6,476.7$	-8,505.5	22,450

$$\Sigma \underset{\sim}{F} = 0 \rightarrow \Sigma F_x = \Sigma F_y = \Sigma F_z = 0$$

$$\Sigma \underset{\sim}{M} = 0 \rightarrow \Sigma Mo_x = \Sigma Mo_y = \Sigma Mo_z = 0 \quad \therefore \begin{cases} R_1 = R_2 = 1,041 \text{ lbf} \\ R_B = R_H = 2,005 \text{ lbf} \\ R_s = 6,412.6 \text{ lbf} \end{cases}$$

F.3. COMPRESSIVE STRESS ON A POST

$$\sigma_{\substack{comp \\ \text{(w/o friction)}}} = 6413/\frac{\pi}{4}(36)$$

$$= 227 \text{ psi*}$$

$$\sigma_{\substack{comp \\ \text{(w/friction)}}} = 6611/\frac{\pi}{4}(36)$$

$$= 234 \text{ psi*}$$

F.4. JAMMED CORE SUPPORT BLOCK

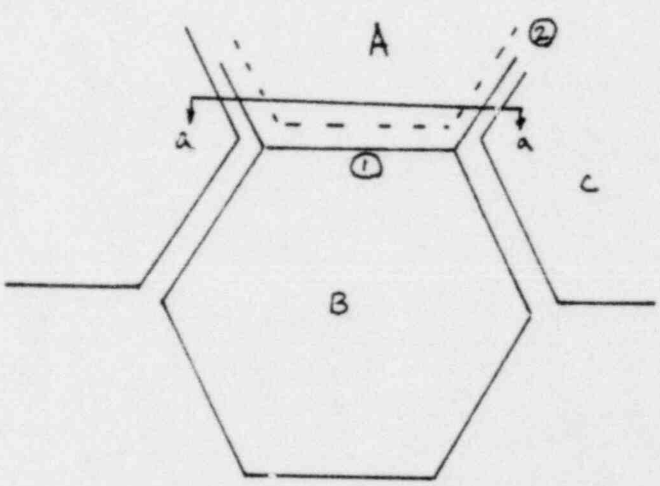

Fig. 22. Plane view of core support block
(Flat face to face contact at 1)

POOR ORIGINAL

---

*With 1 in. offset, additional bending stress is introduced. The load capacity is reduced by 37% to 63% of its original vertical load capacity. See GA-D14137 for some component test results.

As shown in Fig. 22, blocks A and B contact at flat face (1), but face (2) remains without contact. Due to this clearance, the cracked CSB without key rotates until it fills the gap at top and bottom. The analysis given below is approximate.

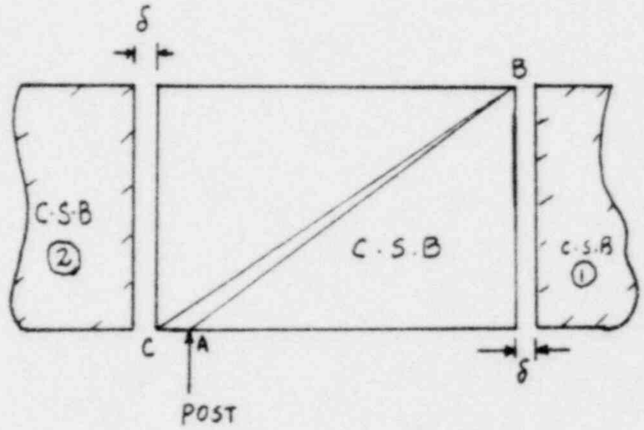

Fig. 23. Profile view of Fig. 22 a-a

where δ = 0.58 in. original gap

AB = radius about post ($\approx$32.58 in.)

CB = 37.65 in.

The following are rotating steps of CSB.

1. CSB rotates about point A until point B touches CSB (1) shown in Fig. 23.

2. CSB slides down until the point C contacts with CSB (2) shown in Fig. 23. This process can be replaced by translating CSB until it touches CSB (2), then rotating about a point A. In this case, the rotation radius will be 37.65 in.

POOR ORIGINAL

Those steps are shown in schematics below.

1. a

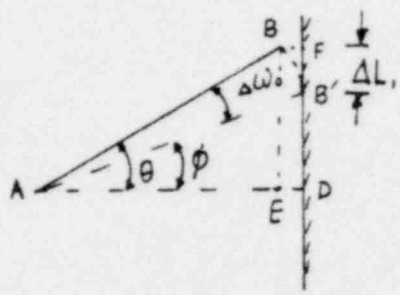

AB = AB´ = 32.58 in.

AE = 23.08 in.

AD = 23.66 in.

$$\theta = \cos^{-1} \frac{23.08}{32.58} = 44.89°$$

$$\phi = \cos^{-1} \frac{23.66}{32.58} = 43.43°$$

$$\Delta\omega_o = \theta - \phi = 44.89 - 43.43 = 1.46°$$

b

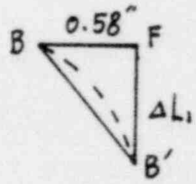

$$BB' = AB \cdot \Delta\omega_o \text{ (Rad)} = 0.83$$

$$\therefore \Delta L_1 = \sqrt{(0.83)^2 - (0.57)^2}$$
$$\cong 0.59 \text{ in.}$$

2. a

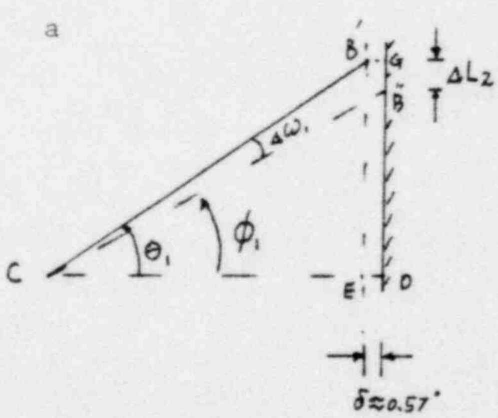

CB˝ = CB´ = 37.65

CE = 30.39

CD = 30.97

$$\theta_1 = \cos^{-1} \frac{30.39}{37.65} = 36.18°$$

$$\phi_1 = \cos^{-1} \frac{30.97}{37.65} = 34.66°$$

$$\Delta\omega_1 = \theta_1 - \phi_1 = 1.52°$$

b

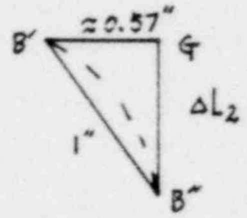

$$B'B'' = (B'C) \times \Delta\omega_1 \text{ (Rad)}$$

$$\cong 1 \text{ in.}$$

$$\therefore \Delta L_2 = \sqrt{1^2 - 0.57^2} = 0.81 \text{ in.}$$

Combining the results in 1 and 2,

$$\text{Total Vertical Displacement} = \Delta L_1 + \Delta L_2$$

$$= 0.59 + 0.81 = 1.4 \text{ in.}$$

$$\text{Total Rotated Angle} = \Delta\omega_0 + \Delta\omega_1$$

$$= 1.46° + 1.52° = 2.98°$$

$$\approx 3°.$$

APPENDIX G

CORE BARREL THERMAL EXPANSION

G.1. RADIAL EXPANSION

The core barrel thermal expansion is calculated as follows:

$$\Delta R = R \times \alpha \times \Delta T$$

where ΔR = radial displacement of core barrel,

R = radius of core barrel,

α = thermal expansion coefficient of core barrel,

ΔT = core barrel differential temperature between normal operation and LOFC maximum temperature.

Using the parameters given in Table 1,

$$\Delta R = \left(\frac{28.14}{2} \text{ ft}\right)\left(\frac{12 \text{ in.}}{\text{ft}}\right) (8 \times 10^{-6}/°F)\ (2300 - 750)°F$$
$$= 2.09 \text{ in.}$$

G.2. GAP CALCULATION OF CSB

Assuming that the radial di·placement is evenly distributed into four spaces, then the gap between CS blocks due to thermal expansion of core barrel is the following:

$$g = \Delta R/4$$

$$= 2.09/4 \cong 0.52 \text{ in.} \approx 0.6 \text{ in.}$$

Total Gap = Normal operation gap + Gap due to core barrel thermal expansion.

$$\text{Gap}_{(\text{total})} = 0.399 \text{ in.} + 0.6 \text{ in.} \cong 1.0 \text{ in.}$$

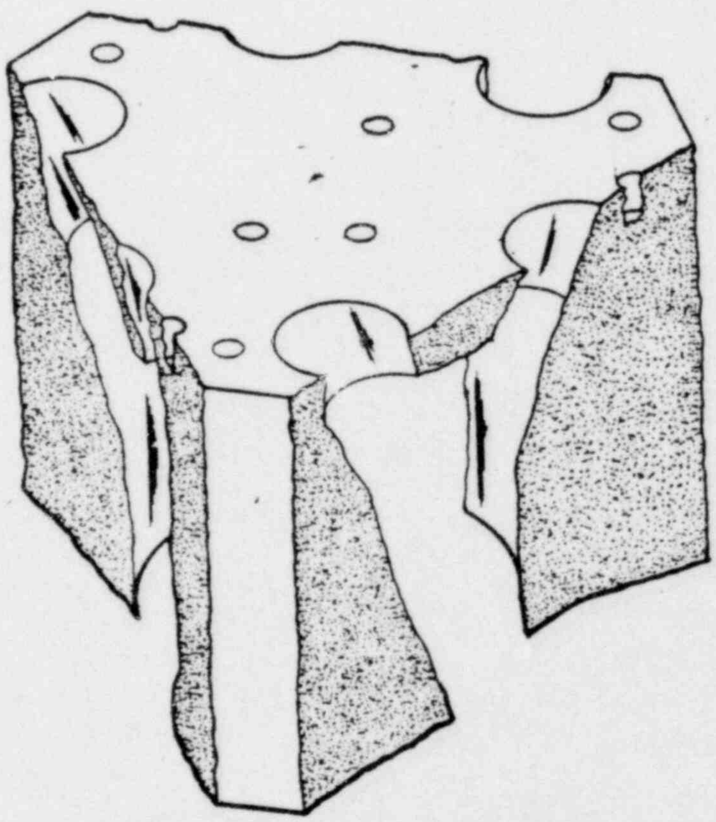

POOR ORIGINAL

Fig. 24. A center piece of cracked CSB

GENERAL ATOMIC COMPANY
P. O. BOX 81608
SAN DIEGO, CALIFORNIA 92138